

## Letter Report (R707)

**Solubility and Speciation Studies of  
Waste Radionuclides Pertinent to  
Geologic Disposal at Yucca Mountain:  
Results on Neptunium, Plutonium and  
Americium in J-13 Groundwater**

***H. Nitsche, E. M. Standifer, S. C. Lee,  
R. C. Gatti, and D. B. Tucker***

**WBS 1.2.3.4.1.4.A  
QA Level II**

**Reporting Period**

**October 1, 1985 – September 30, 1987**

**prepared: September 1987  
revised: January 1988**

**Earth Sciences Division  
Lawrence Berkeley Laboratory  
1 Cyclotron Road  
Berkeley, California 94720**

**DISCLAIMER**

This report was prepared as an account of work sponsored by an agency of the United States Government. Neither the United States Government nor any agency thereof, nor any of their employees, makes any warranty, express or implied, or assumes any legal liability or responsibility for the accuracy, completeness, or usefulness of any information, apparatus, product, or process disclosed, or represents that its use would not infringe privately owned rights. Reference herein to any specific commercial product, process, or service by trade name, trademark, manufacturer, or otherwise does not necessarily constitute or imply its endorsement, recommendation, or favoring by the United States Government or any agency thereof. The views and opinions of authors expressed herein do not necessarily state or reflect those of the United States Government or any agency thereof.

This work was prepared by Nevada Nuclear Waste Storage Investigations (NNWSI) Project participants as part of the Civilian Radioactive Waste Management Program. The NNWSI Project is managed by the Waste Management Project Office (WMPO) of the U.S. Department of Energy, Nevada Operations Office. Lawrence Berkeley Laboratory is operated by the University of California for the U.S. Department of Energy under Contract DE-AC03-76SF00098.

## I. SUMMARY AND RECOMMENDATIONS

We summarize in this letter report solubility studies for the Nevada Nuclear Waste Storage Investigations (NNWSI) project at the Lawrence Berkeley Laboratory (LBL) for the fiscal years 1986 and 1987. The research effort was started October 1, 1985, and is planned to continue at least through FY 1992. It covers the following topics:

1. Summary and Recommendations;
2. Objectives;
3. Concept of Solubility Studies;
4. Design and Fabrication of Equipment;
5. Study of the Solubility and Speciation of Neptunium, Plutonium and Americium in J-13 Groundwater of Varying pH Values and Temperatures of 60° and 90°C;
6. Work in Progress;
7. Reports/Publications/Presentations;
8. Quality Assurance.

### 1.1. Summary

We have studied the solubilities of neptunium, plutonium, and americium in J-13 groundwater from Yucca mountain (Nevada) at three temperatures and hydrogen ion concentrations. They are 25°, 60°C, and 90°C and pH 5.9, 7.0, and 8.5. Tables I, II, and III summarize the results for neptunium, plutonium, and americium, respectively. The results for 25°C are from a study which we did during FY 1984. We included these previous results in the tables to give more information on the solubility temperature dependance; they were, however, done at only one pH (7.0). The solubilities were studied from oversaturation. The nuclides were added at the beginning of each

**Table I. Summary of results for solubility experiments on neptunium in J-13 groundwater at pH 5.9, 7.0, and 8.5, and at 25°, 60°, and 90°C.**

	Steady-state concentration (M)			Oxidation state in supernatant solution		
	25°C	60°C	90°C	25°C	60°C	90°C
pH 5.9	NA	$(6.4 \pm 0.3) \times 10^{-3}$	$(1.2 \pm 0.1) \times 10^{-3}$	NA	V: 100%, 8% carbonate complexed	V: 100%, uncomplexed
pH 7.0	$(1.6 \pm 0.6) \times 10^{-3}$	$(9.8 \pm 1.0) \times 10^{-4}$	$(1.5 \pm 0.5) \times 10^{-4}$	V: 100%, uncomplexed	V: 100%, 15% carbonate complexed	V: 100%, uncomplexed
pH 8.5	NA	$(1.0 \pm 0.1) \times 10^{-4}$	$(8.9 \pm 0.4) \times 10^{-5}$	NA	V: 100%, 84% carbonate complexed	V: 100%, 100% carbonate complexed

	Eh(mV)			Solid phase		
	25°C	60°C	90°C	25°C	60°C	90°C
pH 5.9	NA	$440 \pm 10$	$392 \pm 10$	NA	crystalline, contains carbonate, unidentified	$\text{Np}_2\text{O}_5$
pH 7.0	NA	$325 \pm 10$	$299 \pm 10$	$\text{Na}_3\text{NpO}_2(\text{CO}_3)_2 \cdot \text{nH}_2\text{O}$	crystalline, contains carbonate, unidentified	$\text{Np}_2\text{O}_5$ and a carbonate-containing solid
pH 8.5	NA	$215 \pm 10$	$159 \pm 10$	NA	crystalline, contains carbonate, unidentified	crystalline, contains carbonate, unidentified

**Table II. Summary of results for solubility experiments on plutonium in J-13 groundwater at pH 5.9, 7.0, and 8.5, and at 25°, 60°, and 90°C.**

	Steady-state concentration (M)			Oxidation state in supernatant solution		
	25°C	60°C	90°C	25°C	60°C	90°C
pH 5.9	NA	$(2.7 \pm 1.7) \times 10^{-8}$	$(6.2 \pm 1.9) \times 10^{-9}$	NA	III + poly: $(10 \pm 2)\%$ IV: $(2 \pm 1)\%$ V: $(17 \pm 5)\%$ VI: $(72 \pm 5)\%$	III + poly: $(9 \pm 5)\%$ IV: $(6 \pm 5)\%$ V: $(79 \pm 7)\%$ VI: $(6 \pm 5)\%$
pH 7.0	$(1.6 \pm 0.2) \times 10^{-6}$	$(3.8 \pm 0.8) \times 10^{-8}$	$(8.8 \pm 0.8) \times 10^{-9}$	III + IV + poly: $(2 \pm 3)\%$ V: $(68 \pm 3)\%$ VI: $(27 \pm 9)\%$	III + poly: $(3 \pm 1)\%$ IV: $(2 \pm 1)\%$ V: $(44 \pm 9)\%$ VI: $(52 \pm 4)\%$	no conclusive result
pH 8.5	NA	$(1.2 \pm 0.1) \times 10^{-7}$	$(7.3 \pm 0.4) \times 10^{-9}$	NA	III + poly: $(5 \pm 4)\%$ IV: $(13 \pm 1)\%$ V: $(58 \pm 2)\%$ VI: $(24 \pm 1)\%$	III + poly: $(11 \pm 2)\%$ IV: $(10 \pm 2)\%$ V: $(85 \pm 4)\%$ VI: $(0 \pm 6)\%$

	Eh(mV)			Solid phase		
	25°C	60°C	90°C	25°C	60°C	90°C
pH 5.9	NA	$451 \pm 10$	$360 \pm 10$	NA	mostly amorphous with some crystallinity, contains carbonate and Pu(IV) polymer	
pH 7.0	NA	$386 \pm 10$	$376 \pm 10$	amorphous		
pH 8.5	NA	$241 \pm 10$	$133 \pm 10$	NA		

poly = Pu(IV) polymer

**Table III. Summary of results for solubility experiments on americium in J-13 groundwater, at pH 5.9, 7.0, and 8.4, and at 25°, 60°, and 90°C.**

	Steady-state concentration (M)			Oxidation state in supernatant solution		
	25°C	60°C	90°C	25°C	60°C	90°C
pH 5.9	NA	< $2 \times 10^{-9}$ no steady-state after 168 days	NA	NA	III: 100%	NA
pH 7.0	$(1.1 \pm 0.2) \times 10^{-6}$	< $10^{-8}$ no steady-state after 152 days	NA	III: 100%	III: 100%	NA
pH 8.4	NA	< $5 \times 10^{-9}$ no steady state after 168 days	NA	NA	III: 100%	NA

	Eh(mV)			Solid phase		
	25°C	60°C	90°C	25°C	60°C	90°C
pH 5.9	NA	no steady state, NA	NA	NA	crystalline	NA
pH 7.0	NA	no steady state, NA	NA	$\text{Am}_2(\text{CO}_3)_3 \cdot 2\text{H}_2\text{O}$ and $\text{AmOHCO}_3$	$\text{AmOHCO}_3$	NA
pH 8.4	NA	no steady state, NA	NA	NA	$\text{AmOHCO}_3$	NA

experiment as  $\text{NpO}_2^+$ ,  $\text{Pu}^{4+}$ , and  $\text{Am}^{3+}$ .

The neptunium solubility decreased with increasing temperature and with increasing pH. The soluble neptunium did not change oxidation state at steady state. The pentavalent neptunium was increasingly complexed by carbonate with increasing pH. All solids were crystalline and contained carbonate, except the solid formed at 90°C and pH 5.9. We identified this solid as crystalline  $\text{Np}_2\text{O}_5$ . The 25°C, pH 7 solid was  $\text{Na}_3\text{NpO}_2(\text{CO}_3)_2 \cdot \text{nH}_2\text{O}$ .

Plutonium concentrations decreased with increasing temperature and showed no trend with pH.  $\text{Pu(V)}$  and  $\text{Pu(VI)}$  were the dominant oxidation states in the supernatant solution; as the amount of  $\text{Pu(V)}$  increased with pH,  $\text{Pu(VI)}$  decreased. The steady-state solids were mostly amorphous, although some contained a crystalline component. They contained  $\text{Pu(IV)}$  polymer and unknown carbonates.

We could not determine steady-state concentrations for the 60°C americium experiments within five months. The high specific  $\alpha$ -activity of the americium solution probably caused this problem. The americium supernatants did not change oxidation state. We identified the solubility-limiting solids as  $\text{AmOHCO}_3$ , with a mixture of  $\text{Am}_2(\text{CO}_3)_3 \cdot 2\text{H}_2\text{O}$  in the 25°C, pH 7 solid. The compound formed at 60°C and pH 5.9 was crystalline and is currently under analysis.

## 1.2. Recommendations

1. We must identify the remaining unknown solids. A first step toward their identification is elemental analysis. We will characterize the unidentified solids by neutron activation or x-ray fluorescence analysis.
2. We have developed a scheme to determine the oxidation states of plutonium in trace-level solutions. This method is, however, an indirect determination. It converts the plutonium complexes to plutonium ions which are then isolated and measured. A direct speciation method would give us additional knowledge on

solution complexation. Laser-induced photoacoustic spectroscopy (LPAS) seems well suited to solve this problem.

3. We need steady-state concentrations for the americium experiments at 60° and 90°C. We attribute the problems in the 60°C study to  $\alpha$ -induced damage of the solubility container. This damage released particles into the solution on which americium pseudocolloids probably formed. To reduce the radiation level, we will replace the  $^{243}\text{Am}$  with the stable lanthanide neodymium. Neodymium has similar properties to americium, including nearly identical ionic radii and valency. Additionally, neodymium carbonates and hydroxycarbonates are well characterized. We should be able to get steady-state concentrations from neodymium solubility studies. Because of the similarity between the two elements, the results for neodymium also apply to americium.
4. We plan to measure the solubilities of neptunium, plutonium, and americium in UE25p#1 groundwater. This water has a higher ionic strength than J-13 water, which could affect the solubilities. These experiments will be performed at 25° and 60°C and pH values of 6, 7, and 8.5.
5. To determine the influence on the solubilities of the complexing ions in groundwaters from Yucca Mountain, we will do control experiments in non-complexing electrolyte. Temperature and pH conditions should be the same as those for the groundwater experiments.
6. We need to know if the oversaturation solubility experiments have indeed reached equilibrium, and not merely steady state. Approaching equilibrium from undersaturation should yield the same results as from oversaturation if a true equilibrium is reached. We plan to synthesize the solubility compounds from the oversaturation experiments and dissolve them under identical conditions in undersaturation experiments.

7. Alpha-radiation can affect the solubility of waste elements by altering the composition of the water and by changing the crystallinity of the solids that form. To monitor this effect, we will use two  $\alpha$ -emitting isotopes of the same element that have significantly different half-lives (e.g.,  $^{239}\text{Pu}$  versus  $^{242}\text{Pu}$ ).
8. We recommend the expansion of solubility studies to other waste radionuclides. Important waste elements with solubility-limited concentrations are uranium, thorium, radium, nickel, and zirconium.

## 2. OBJECTIVES

This study determines the solubilities and the oxidation state distributions (whenever possible the speciation) of waste elements in groundwaters of the potential repository at Yucca Mountain.

Radiation-induced heat can generate elevated temperatures at the repository. Possible chemical interaction of groundwater flowing through the repository with the backfill material and/or the canister material can alter the pH value of the groundwater. As a consequence of these conditions, this study will investigate the effects of temperature and pH changes on the solubilities and speciation of waste element solutions.

The data will be used as input to model radionuclide transport from the repository.

These data will also be compared with solubilities calculated by the EQ 3/6 Chemical Equilibrium Code which is used to model waste element solubilities in the NNWSI Project. Possible discrepancies between measured solubilities and speciation and results from modeling calculations may indicate necessary improvements for the EQ 3/6 thermodynamic data base.

### 3. CONCEPT OF SOLUBILITY STUDIES

We are following the guidelines of the U.S. Nuclear Regulatory Commission (NRC). The NRC has issued a Technical Position "Determination of Radionuclide Solubility in Groundwater for Assessment of High-Level Waste Isolation", which outlines the concept of solubility studies.<sup>0</sup>

Equilibrium solubility conditions for a given element can exist when a solid containing the element is in contact with the solution. Maximum aqueous solution concentrations of the element are controlled by the most stable solid participating in reactions with aqueous species of the element. Other solids of the element that would lead to higher solubilities under the experimental conditions should dissolve because they are less stable than the solid that controls solubility.

#### 3.1. Oversaturation vs. Undersaturation

Ideally, solubility experiments should approach solution equilibrium from oversaturation and undersaturation. Approach from oversaturation requires adding an excess amount of the element in soluble form to the aqueous solution and then monitoring the precipitation of insoluble material until equilibrium is reached. The solid formed must then be isolated and characterized. Approach from undersaturation requires a prepared, well-defined solid. The solid is then allowed to dissolve in aqueous solution until equilibrium is reached. For both cases the solution concentration is measured as a function of time until equilibrium conditions are reached.

Solution kinetics will control the equilibrium speed in a solubility experiment. Some solutions equilibrate fast, some slower. It must be demonstrated that equilibrium is reached. This is experimentally determined (for both oversaturation and undersaturation experiments) by measuring the solution concentration as a function of time. When the concentration stays constant for several weeks, it is assumed that equilibrium was established. Because this assumption is based on judgment, the term steady state

instead of equilibrium is more precise. The NRC defines steady state as "the condition where measurable changes in concentrations are not occurring over practical experimental times."<sup>10</sup> At steady state, thermodynamic forces may still change the solution composition: solids will become less soluble as they change from a higher to a lower free energy. The change may be very slow and may not show in experiments even after several years. Infinitesimal changes may require infinite experimental times.

Despite this restriction, time-limited laboratory solubility experiments can supply valuable information. They provide good estimates on the upper limit of radionuclide concentrations in solution. The experimentally-determined steady-state concentrations would be higher than the equilibrium concentrations.

A reliable method to prove that a steady state was reached is to approach equilibrium from oversaturation and undersaturation. When the solution concentrations are equal from the two independent experiments, the data are very reliable.

For this solubility study, we will attempt to approach steady-state concentrations from both undersaturation and oversaturation. First, we will do experiments approaching steady-state concentrations from oversaturation and we will characterize the solids that form. This procedure has the advantage of not specifying the solid that controls solubility, but of allowing the system under investigation to determine the solid that will precipitate. Then, we will prepare these solids and use them for experiments that approach steady state from undersaturation.

### 3.2. Phase Separation

Phase separations must be as complete as possible for these experiments. The separation of the solid from the solution often represents a significant practical problem for solubility measurements. Higher or lower apparent solubilities, compared to the steady-state values, can result from incomplete phase separation or from sorption of solute during and after the separation. Incomplete phase separations, that is, leaving

some of the solid with the solution phase, would lead to higher waste element solubilities. Lower solubilities would be measured if constituents of the steady-state solution were sorbed on filters during a filtration and on container walls after the separation.

Experimentally, the solids and solutions are separated based on differences in size (via filtration) or density (via sedimentation or centrifugation). Filtration is the more commonly applied technique since it physically partitions the solute and solids. Ultrafiltration, i.e., filtration using membranes  $\leq 0.1 \mu\text{m}$ , can effectively remove colloidal particles from aqueous solution. Colloids are solids of an element under investigation that are more stable than the solid controlling solubility under the given experimental conditions, but which may not participate in the solubility equilibrium because precipitation or dissolution kinetics may be too slow. A potential problem with ultrafiltration is adsorption of soluble species on ultrafiltration membranes. Effective filters for solubility studies must pass soluble species through the filter quantitatively; that is, the filter either has no active sorption sites or any such sites on the membrane must be irreversibly blocked.

We will experimentally verify the most effective filtration methods for each nuclide that we study. We will judge filters to be adequate if they have a small enough pore size to retain the solids and colloids, and if they also show no or only minimal sorption during multiple filtrations. These tests do not attempt to determine the filter sorption equilibrium. They are only made to find filters which do not disturb the solution equilibrium during the filtration.

### 3.3. Identification of Solids

The identification of the solid formed in the solubility test is very important. Thermodynamically meaningful results require the existence of a well-defined solid phase which generally consists of crystalline material. The solids formed in solubility tests from oversaturation must be clearly identified by physical or chemical

characterization methods. Only when identified unambiguously can the solid be synthesized for use in undersaturation solubility tests. We will identify the solids by x-ray powder diffraction analysis, Fourier transform infrared-spectroscopy (FTIR), and neutron activation analysis (NAA).

### 3.4. Determination of Oxidation States and Speciation

The oxidation state in solution describes the charge of soluble species, and speciation describes their nature. Radionuclides can have one single or several different oxidation states in solution. They can be present as simple ions or as complexes. When the ions react with one or several other solution components, they can form soluble complexes.

Information on oxidation states and speciation is important for transport models simulating migration and sorption along the flow path. The charge and speciation of radionuclides will control their adsorption and transport in the geologic host.

Oxidation states and speciation in solution are commonly determined by (a) absorption spectrophotometry, (b) ion-exchange chromatography, (c) solvent extraction, (d) coprecipitation technique, and (e) electrochemistry. Of these different methods, only absorption spectrophotometry can provide information on speciation, while the others identify only the oxidation state in solution.

Absorption spectrophotometry has a detection limit of about  $10^{-6}$  M. This relatively high concentration limits spectrophotometry for speciation determination in solutions from radionuclide solubility studies. The solubilities can be several orders of magnitude below  $10^{-6}$  M. Recently, several research groups used photocoustic spectroscopy for the oxidation state-specific detection and speciation of actinide ions in aqueous solution. For example, the method detects plutonium species at  $10^{-8}$  M, and americium species even at  $10^{-9}$  M. The detection limit improves by two to three orders of magnitude compared with conventional absorption spectrophotometry.

As in conventional spectrophotometry, photoacoustic spectroscopy measures the energy absorbed when light passes through the sample. The difference is in the measurement of the absorbed energy. Spectrophotometry measures the energy difference by comparing the light intensity of a sample beam with a reference beam. Photoacoustic spectroscopy measures the absorbed energy directly as a pressure wave in solution. Actinide ions in solution generate this pressure wave by the non-radiative decay of the 5f electron to the ground state; the pressure is proportional to the absorbed energy.

The methods listed above as (b) to (e) determine only the oxidation state in solution, because they cannot determine species. They detect the oxidation state of ions indirectly. This is different from absorption spectrophotometry, which detects the solution species directly. The indirect methods, however, detect very small concentrations ( $10^{-10}$  M and below), which is useful for radionuclide solubility studies. Solvent extraction and coprecipitation are often used successfully to determine the oxidation states of ions in very dilute solutions. Ion exchange chromatography is less reliable for this purpose, because the exchange resin often reduces the solution ions. This gives wrong results for the oxidation state distribution. Electrochemical detection reduces or oxidizes the solution ions and measures the potentials of the reduction and oxidation reactions, respectively. The potential then identifies the individual ion. Electrochemistry needs fast kinetics and reversible thermodynamics for the reduction or oxidation step. This limits the method very much, because many radionuclide ion reactions are irreversible and slow (e.g.,  $\text{NpO}_2^+/\text{Np}^{4+}$ ,  $\text{PuO}_2^+/\text{Pu}^{4+}$ ).

We will determine the oxidation state of species in solution by a solvent extraction and coprecipitation technique. We will also try to determine the nature of the solution species by spectrophotometry when the solution concentration is greater than  $10^{-6}$  M.

The sensitivity of our analytical methods limits this study. We need photoacoustic spectroscopy (LPAS) to determine directly the species in the supernatant solutions

of the solubility experiments at sub-micromolar concentrations.

### 3.5. Radiation

Radiation can affect the solubility of waste elements by altering the composition of the water and/or by altering the crystallinity of the solids that form. The primary effects of alpha radiation are a change in pH and a trend towards more oxidizing conditions in the water. Solids of alpha-emitting elements tend to show self-irradiation damage to their crystal structure. We will investigate the effects of alpha radiation on solubility by using actinide isotopes that are present in high-level waste. We will use two isotopes of the same element which are significantly different in their specific alpha activity for selected solubility experiments. For example,  $^{239}\text{Pu}$  has 15.6 times the specific activity of  $^{242}\text{Pu}$ , and  $^{241}\text{Am}$  is 17 times more radioactive than  $^{243}\text{Am}$ . Because the range of alpha particles is very short, we will not study the effects of alpha radiation on the solubility of coexistent waste elements that are not alpha emitters. The effect of alpha radiation on the water composition will be considered in defining the ranges of water composition that will be employed for solubility measurements.

We will not consider the effects of gamma radiation on solubility, because gamma radiation levels will be reduced considerably by the end of the containment period. Possible influences of the remaining gamma radiation levels on the water composition are being covered by the water compositions already considered.

## 4. DESIGN AND FABRICATION OF EQUIPMENT

### 4.1. Controlled Atmosphere Glove Box

Due to the radiation hazard of the actinide elements under investigation, all experimental work must be performed in glove boxes. External CO<sub>2</sub>-control of the experimental solutions requires the exclusion of atmospheric CO<sub>2</sub>. To satisfy both

conditions, we use a controlled atmosphere glove box. The glove box was installed, equipped, and shake-down tested.

#### **4.2. Control System for pH and Temperature**

The report titled "Data Acquisition and Feedback Control System for Solubility Studies of Nuclear Waste Elements" (LBL-23541) was prepared by D. B. Tucker, E. M. Standifer, R. J. Silva, and H. Nitsche. This report is currently under NNWSI-Policy Review and will be submitted for publication to the journal *Analytical Chemistry*.

Because the solubilities are highly sensitive to pH and temperature changes, close control of these parameters is necessary. We designed a computer-operated control system (pH-stat) to maintain the aqueous actinide solutions at constant temperatures and pH values for the solubility experiments. The pH-stat records and adjusts the pH values of the experimental solutions (groundwater or non-complexing electrolyte) at the target values with standard deviations not exceeding 0.1 pH unit. It uses small amounts (usually between 5 to 50 microliters) of diluted (0.05 – 0.1 M)  $\text{HClO}_4$  or  $\text{NaOH}$  solution for the pH adjustments. We do not expect any substantial change of the water chemistry from this adjustment. Temperatures from 25° to 90°C can be controlled within less than 1°C.

#### **4.3. Pressure Control System**

We designed and manufactured four identical pressure regulation systems. These systems are used to maintain the well waters used in experiments at their nominal carbonate concentrations when their temperatures and pH values are adjusted to conditions differing from their natural state. The system also ensures that no significant evaporative loss of the solutions can occur at elevated temperatures.

#### **4.4. Digital Multichannel Pulse Height Analyzing System**

A low-energy germanium  $\gamma$ -x-ray detector was manufactured. A personal computer (PC)- driven digital multichannel analyzer system was interfaced with the detector and tested. The manufacturer-supplied post-processing software was unsatisfactory for our applications. We developed and tested new post-processing software and we verified the software to produce results acceptable for our research use.

#### **4.5. Digital Absorption Spectrophotometer**

A portable, PC-controlled spectrophotometer was acquired and tested. The unit has remote measuring capability via fiber optics. We developed some improved post-processing software, which we tested to produce acceptable results.

### **5. STUDY OF THE SOLUBILITY AND SPECIATION OF NEPTUNIUM, PLUTONIUM, AND AMERICIUM IN J-13 GROUNDWATER OF VARYING pH VALUES AND TEMPERATURES OF 60° AND 90°C**

#### **5.1. Experimental**

We studied the solubilities of neptunium, plutonium and americium at 60° and 90°C and respective pH values of 5.9, 7.0, and 8.5. Measurements were made in an inert-atmosphere box to avoid contamination of solutions by atmospheric CO<sub>2</sub>. The solubilities were studied from oversaturation by injecting a small amount, usually between 0.5 and 1 ml, of actinide stock solution into 50 ml of groundwater obtained from Well J-13. The analysis of the water composition is listed in Table IV.

**Table IV. Well J-13 water composition.<sup>2</sup>**

Species	Concentration mM
Ca	0.29
Mg	0.072
Na	1.96
K	0.136
Li	0.009
Fe	0.0008
Mn	0.00002
Al	0.0010
SiO <sub>2</sub>	1.07
F <sup>-</sup>	0.11
Cl <sup>-</sup>	0.18
SO <sub>4</sub> <sup>2-</sup>	0.19
NO <sub>3</sub> <sup>-</sup>	0.16
Alkalinity	2.34 mequiv/L
pH	7.0
Eh	700 mV

### 5.1.1. Solutions

$^{237}\text{Np(V)}$  and  $^{243}\text{Am(III)}$  stock solutions were prepared by dissolving their oxides in HCl.  $^{239}\text{Pu(IV)}$  stock was prepared from plutonium metal. The actinide solutions were purified from possible metal contaminants by ion exchange chromatography. For neptunium and plutonium anion exchange was used, while cation exchange was employed for americium. The purity of these stock solutions was tested by spark emission spectroscopy and no contaminants were found above the detection limits of the method. The solutions were converted to a non-complexing perchlorate system. The neptunium and plutonium stock solutions were in the oxidation state +6 after their conversion to perchlorate and were reduced electrolytically to  $\text{NpO}_2^+$  and  $\text{Pu}^{4+}$ , respectively. Valence purity was established by absorption spectrophotometry. Details for the preparation of actinide stock solutions were previously published elsewhere.<sup>1</sup>

The groundwater, actinide stock solutions, and all other solutions utilized in this experiment were filtered through 0.22  $\mu\text{m}$  polyvinylidene difluoride syringe filter units (Millipore Corp., Bedford, MA). Filtration was used to remove suspended particulate material, e.g., dust or silica, that could absorb the actinide ions to form pseudocolloids. Before the addition of actinide stock solutions to the J-13 samples, a small amount of  $\text{CO}_2$ -free sodium hydroxide solution was added to the J-13 samples in order to keep the pH values at or above the desired solution pH. Letting the pH drop below the target value would necessitate addition of concentrated base to the system while the actinide ion is already present in the solution. Addition of strong base can result in unpredictable microprecipitation and formation of microcolloids.

The well water's total dissolved carbonate ( $2.34 \times 10^{-3}$  M) was preserved at each individual pH and temperature by equilibrating the solution with mixtures of  $\text{CO}_2$  in argon. The amount of  $\text{CO}_2$  at a given pH and temperature was calculated from Henry's constant and the dissociation constants of carbonic acid from literature data.<sup>3</sup> If the value at the given ionic strength and temperature was not available, the number

was derived by interpolation of adjacent values. For the 60°C experiment, the total dissolved carbonate was held constant at the targeted pH values of 5.9, 7.0, and 8.5 by respective mixtures of 9.67%, 2.35%, and 0.0877% CO<sub>2</sub> in argon. For the 90°C series, mixtures of 18.58%, 4.05% and 0.142% CO<sub>2</sub> were used for the solutions of pH 5.9, 7.2, and 8.5, respectively.

The test solutions were kept in 90 ml PTFE cells with sealed ports at the top. The ports accommodate the permanent emplacement of a pH electrode, an opening to draw samples, and three 1/16" diameter Teflon lines for addition of acid, base, and the CO<sub>2</sub>-argon mixture. The temperature was controlled by placing the test cells in a heated aluminum block of LBL design. The electric heater was mounted on an orbital shaker (Lab-Line Inc., Melrose Park, IL) and all solutions were shaken continuously at approximately 100 rpm. The solutions' pH values were controlled by a computer-operated pH control system (pH-stat). The pH-stat was designed and assembled at LBL. It records and adjusts the pH values automatically over the required long periods of time with standard deviations generally not exceeding 0.1 pH unit. We prepared a report, which is currently undergoing NNWSI Policy Review, describing this unit in detail.<sup>4</sup> We could not use the pH-stat for the 90°C experiments. The combination pH electrodes (Beckman Instr. Inc., Model 39522), used at 60°C to monitor the solutions pH values, deteriorated rather rapidly when in contact with the 90°C solutions. The deterioration is mainly due to the dissolution of the Ag/AgCl layer of the reference electrode wire and also of the wire used in the pH sensing compartment itself; the solubility of AgCl increases approximately 240 times when the temperature changes from 10° to 100°C. Although the manufacturer claims the working range of these electrodes is up to 100°C, we cannot use the electrodes continuously with the pH-stat. Therefore, we performed the pH adjustment every day by hand: the electrodes were removed from the individual experimental solutions after each adjustment and reintroduced for each new measurement. Before measuring the pH, the electrodes

were calibrated and remained in the solutions for several hours to come to temperature equilibrium. This method of controlling the solutions pH values was so time-consuming that we had to stop the americium solubility experiments in order to attend to the other solutions properly. We are currently testing Ross combination electrodes from Orion which have a  $I_2/2I^-$  reference electrode and platinum wires. If proven sufficient, we must redesign the solubility cells to accommodate these electrodes; they have different dimensions than the Beckman electrodes.

### 5.1.2. Phase Separation

Achievement of steady-state conditions for the solubility measurements was monitored by sampling aliquots of the solution phases and analyzing for the respective radioisotope as a function of time. We studied the effect of phase separation on the measured solubilities at 60° and 90°C. We routinely employed Centricon-30 centrifugal filters (Amicon Corp., Danvers, MA) with minimal sorption to separate the phases of the neptunium and plutonium solutions. The filters contain a YM-type membrane with a calculated pore size of 4.1 nm. To minimize possible radionuclide adsorption on the filter, a presaturation step was carried out. The separations for the americium solutions had problems. We describe results of the separation studies at 60°C for neptunium, plutonium, and americium in a separate report, which is currently under NNWSI Policy Review.<sup>5</sup> The results for 90°C test are described below. The tests were designed to evaluate the effectiveness in separating solids from the solution phase for different filters. Although the sorption characteristics of these filters have been tested at ambient temperature, no performance data are available at our experimental temperatures of 60° and 90°C.<sup>1</sup>

We tested radionuclide sorption onto the filters by taking a sample from the supernatant of the solubility test solution after it was settled by gravity for one hour. The sample was split. While one part was assayed, the remaining fraction was filtered

through the filter to be tested. After a sample was removed from the filtrate for counting, the remaining filtrate was recycled through the filter. A filter which readily sorbs a soluble nuclide would show decreasing nuclide concentration in filtrates filtered  $n$  times relative to those filtered  $n-1$  times until the filter sorption sites were saturated.

At 90°C, tests for neptunium and plutonium were conducted using Centricon-30 filter units and Nuclepore 200 nm membranes mounted in Sartorius 13 mm syringe filter holders. The results for neptunium are shown in Figure 1. The concentration at zero number of times filtered is the concentration of the unfiltered solution after gravity settling for one hour. One on this axis is the solution concentration after the first filtration. Two is the concentration after the second filtration through the same filter. We conclude from these experiments that both filters tested display minimal sorption of soluble neptunium at the pH. Furthermore, both filter sizes provide adequate separation between solution and solid phase. For reasons of experimental ease, we continued to use the Centricon-30 centrifugal filters for the neptunium experiment. Although the sorption experiments have shown no significant neptunium adsorption, we pre-saturated the filters for all neptunium solubility determinations, because we did not know the results of this study, which we did near the end of the solubility experiments.

The results for plutonium are shown in Figure 2. The meaning of the x-axis labelling is the same as for neptunium. At pH 8.5, both filters displayed no significant sorption; the concentration after the second filtration was the same as after the first filtration. The filter with the larger pore size (200 nm) transmitted plutonium yielding an about ten thousand times higher measured solubility than that measured with the 4.1 nm filter. This shows that, in agreement with the 60°C experiment, a major fraction of the solid plutonium was between 4.1 and 200 nm; it remained suspended in solution after one hour of gravity settling.

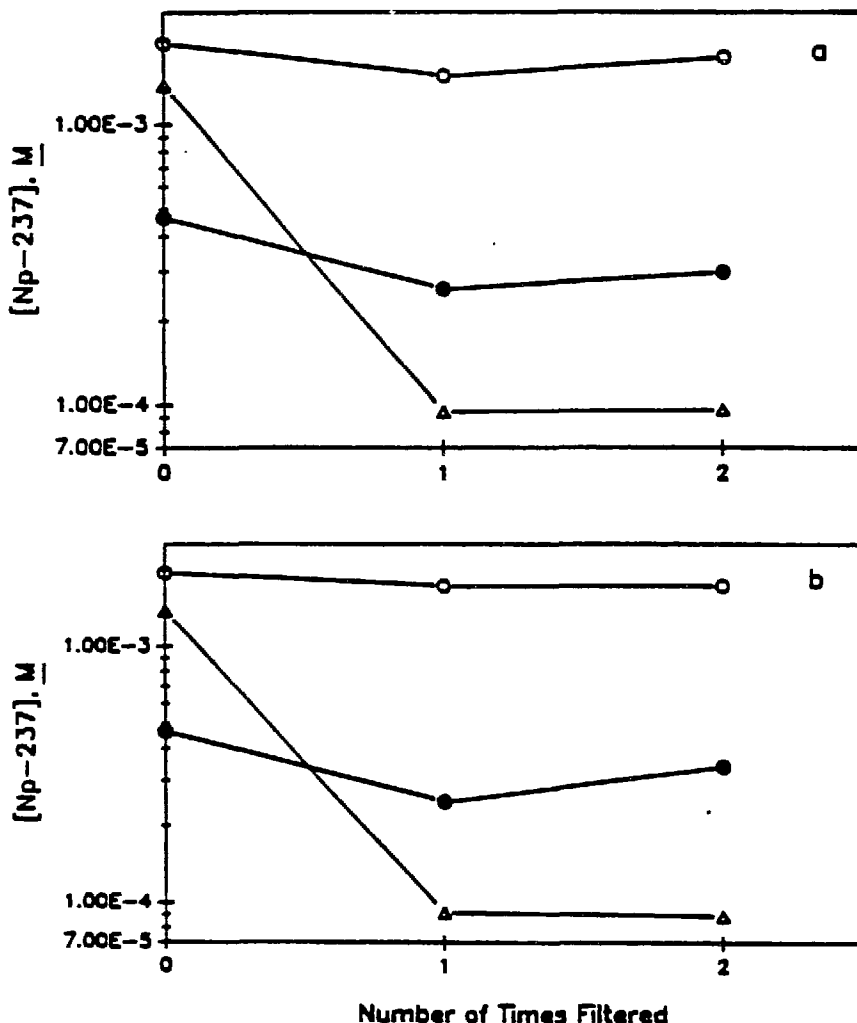


Figure 1. Results of filtration experiments of Np in J-13 groundwater at 90°C and at pH 5.9, 7.2, 8.4. (a) Amicon 4.1 nm, (b) Nuclepore 200 nm. pH 5.9 (open circles), pH 7.2 (filled circles), pH 8.4 (triangles).

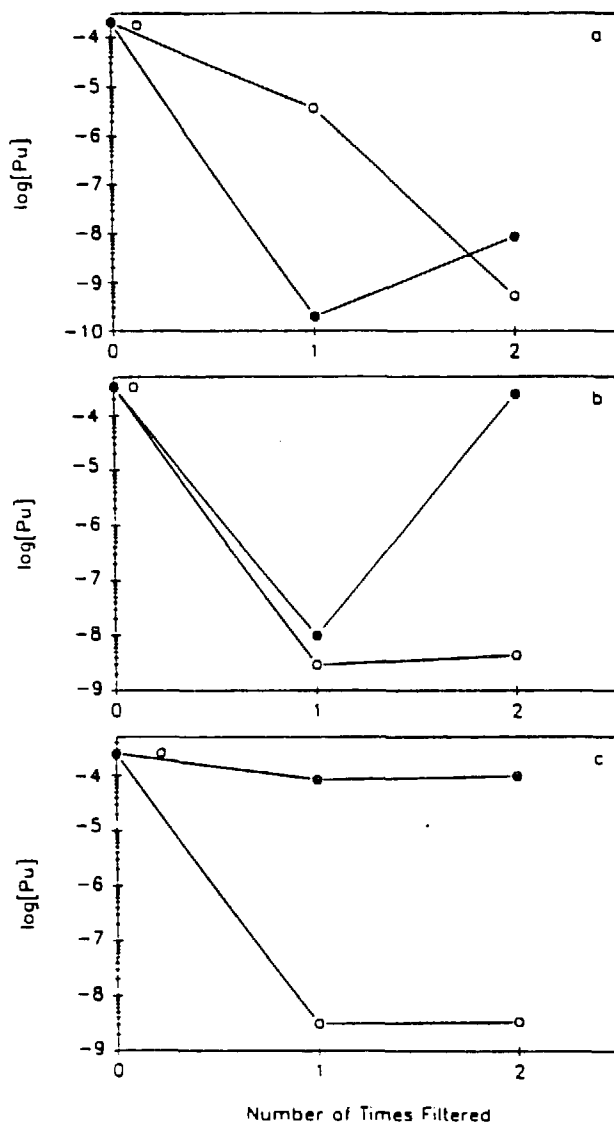


Figure 2. Results of filtration experiments of Pu in J-13 groundwater at 90°C and at pH values of (a) 5.9, (b) 7.0, and (c) 8.5. Amicon 4.1 nm (open circles), Nuclepore 200 nm (filled circles).

At pH 7.2 the Amicon filter showed no significant absorption. The concentration after the second filtration even increased somewhat. This is probably due to evaporative concentration during the 15 minute filtration by centrifugation; the centrifugal filters were very difficult to seal. The first Nuclepore filtration also indicated that particles larger than 200 nm remained in solution after the gravity settling. This conclusion, however, was drawn from only one filtration, because the filter probably leaked during the second filtration; this explains the large concentration increase.

At pH 5.9 the experiment was ambiguous for sorption on either filter and a repetition of the test was impossible because no further solution was available. Nevertheless, the relatively stable plutonium concentrations determined throughout the solubility experiment at this pH showed that the method of separation is internally consistent.

### 5.1.3. Analysis

After separation of the solution and the solid phases, the two components were analyzed separately. Concentration measurements of the supernatants were made by counting liquid aliquots with a germanium low-energy counting system (LBL design). For  $^{237}\text{Np}$  and  $^{243}\text{Am}$  the 29.38 keV and the 74.67 keV  $\gamma$ -ray lines were used, respectively. A waiting period of at least 30 days was required for the  $^{243}\text{Am}$  samples before they could be assayed since the  $^{243}\text{Am}$  was not at secular equilibrium with the  $^{239}\text{Np}$  daughter at sampling. After this time, the 74.67 keV  $\gamma$ -line was resolved from the large Compton edge of the plutonium *K* x-rays and the 106.13 keV  $\gamma$ -line from the  $^{239}\text{Np}$  decay.

$^{239}\text{Pu}$  was analyzed by utilizing the *U L* x-rays coming mainly from the decay of  $^{238}\text{Pu}$ ,  $^{240}\text{Pu}$ , and  $^{242}\text{Pu}$ , which were also present in small quantities in the  $^{239}\text{Pu}$  solutions. Possible contributions to the *L* x-rays from the decays of other radionuclides, also present in small amounts, were corrected by subtraction. The method is summarized in a detailed report which will be submitted for NNWSI Policy Review.<sup>6</sup> In

selected cases, liquid scintillation counting was also used for plutonium concentration determinations (Packard Instr. Co., Dowers Grove, Ill., model Tri-Carb 460C). The two energy windows of the counter were set to properly discriminate between possible  $\beta$ -emitting solution contaminants and the plutonium  $\alpha$ -radiation. Repeated sample counting and the observation of a constant count rate in the  $\alpha$ -window ensured no  $\beta$  contribution to the  $\alpha$ -count.

#### 5.1.4. Eh Measurements

At the end of each solubility experiment, we measured the Eh with a platinum electrode versus a Ag/AgCl/sat. NaCl reference. We cleaned the platinum electrode with 6 M HNO<sub>3</sub> before and after each measurement. Readings were stable within 30 to 60 minutes. The electrode setup was checked with "Zobell Solution" before and after each measurement.<sup>7,8</sup>

#### 5.1.5. Identification of Solids

The solid compounds were analyzed by x-ray powder diffraction measurements. A few micrograms of each actinide precipitate were placed in a 0.33 mm diameter quartz capillary tube, and the tube was sealed with an oxy-butane microtorch. The tube was mounted in an 11.46 cm diameter Debye-Scherrer camera and then irradiated with x-rays from a Norelco III x-ray generator (Phillips Electronics, Inc.). Copper K<sub>α</sub> radiation filtered through nickel was used. When the solids did not produce any pattern or when the pattern could not be assigned to any known compound, Fourier transform infrared-spectroscopy (FTIR) was applied. A small amount of each solid was placed between two pre-fabricated polished KBr windows, and the windows were then sealed at the rim with epoxy. Great care was taken to keep the outside of the KBr windows free of contamination. These samples were then analyzed by FTIR (Mattson Instr., Inc., Madison, WI, model Sirius 100). Neutron Activation Analysis

(NAA) will give additional information on the stoichiometry of the unidentified precipitates. This analysis is currently being performed for the 60°C experiments and the 90°C solids will follow.

## 5.2. Results and Discussion

### 5.2.1. Neptunium

#### 5.2.1.1. Solubility

Figures 3 and 4 show the results of the solubility measurements as a function of equilibration time and pH for 60° and 90°C, respectively. The steady-state concentrations and the solutions' Eh values are given in Table V. The neptunium solubility decreased with increasing temperature and with increasing pH.

#### 5.2.1.2. Speciation

The supernatant solutions were analyzed by absorption spectrophotometry to determine the oxidation state and speciation. The spectra are shown in Figures 5 and 6 for 60° and 90°C, respectively. The supernatant sample from the experiment at pH 5.9, 60°C was diluted with J-13 water to keep the absorbance value within the sensitivity limit of the spectrophotometer used. All three spectra from the 60°C experiment show the  $\text{NpO}_2^+$  main absorption band at 980 nm and an additional band at 992 nm – increasing with pH – which is due to carbonate complexation.<sup>1</sup>

From the difference between the total amount of neptunium – determined by  $\gamma$ -spectroscopy – and the free  $\text{NpO}_2^+$  – determined from the 980 nm peak – the amount of neptunium present as carbonate complex was determined to be:

8% for pH 5.91,

15% for pH 7.01, and

84% for pH 8.48.

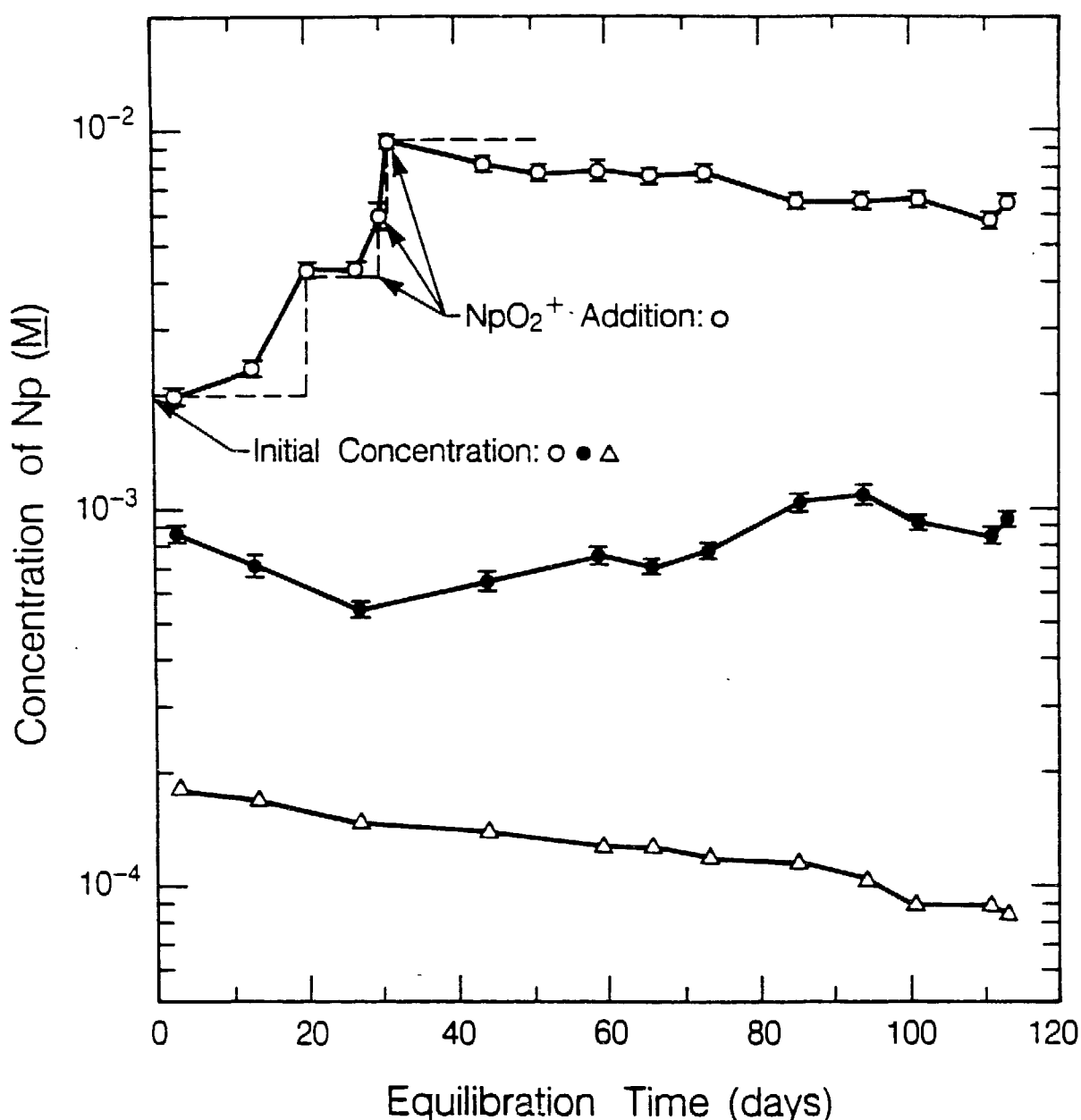


Figure 3. Solution concentrations of  $^{237}\text{Np}$  in contact with precipitate obtained from supersaturation in J-13 groundwater at  $60^\circ\text{C}$  as a function of time.  $\text{pH } 5.9 \pm 0.1$  (open circles),  $\text{pH } 7.0 \pm 0.1$  (filled circles), and  $\text{pH } 8.5 \pm 0.1$  (triangles). The neptunium was added initially (day 0) as  $\text{NpO}_2^+$ . For the solution at  $\text{pH } 5.9$ , additional neptunium additions were necessary to reach supersaturation.

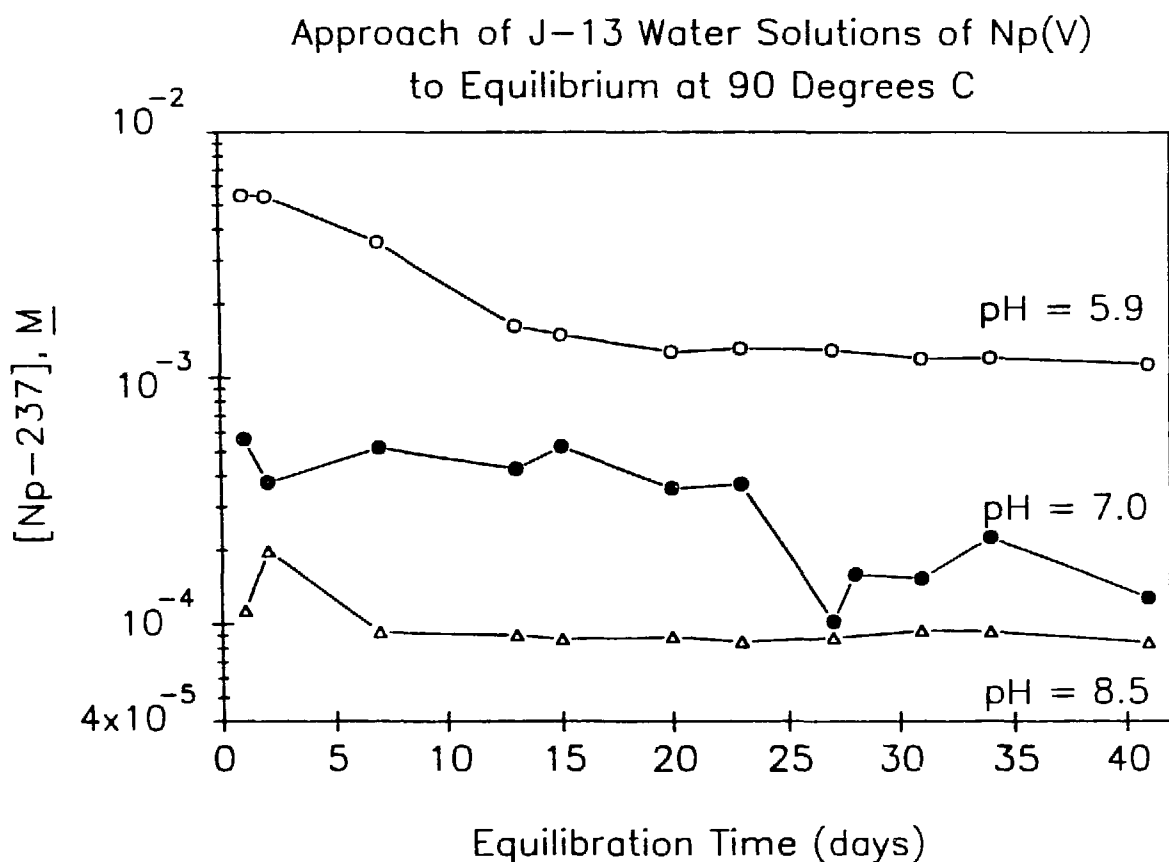


Figure 4. Solution concentrations of  $^{237}\text{Np}$  in contact with precipitate obtained from supersaturation in J-13 groundwater at 90°C as a function of time. pH 5.9  $\pm$  0.2 (open circles), pH 7.2  $\pm$  0.2 (filled circles), and pH 8.4  $\pm$  0.1 (triangles). The neptunium was added initially (day 0) as  $\text{NpO}_2^+$ ; initial concentrations were  $8.71 \times 10^{-3}$  M (pH 5.9),  $2.01 \times 10^{-3}$  M (pH 7.2), and  $1.85 \times 10^{-3}$  M (pH 8.4).

**Table V. Comparison of steady-state solution concentrations for Np in J-13 groundwater at 60° and at 90°C.**

Np	60°C			90°C		
	pH	conc. (M)	Eh (mV vs. NHE)	pH	conc. (M)	Eh (mV vs. NHE)
5.9 ± 0.1	(6.4 ± 0.3) × 10 <sup>-3</sup> <sup>a</sup>	440 ± 10	5.9 ± 0.2	(1.2 ± 0.1) × 10 <sup>-3</sup> <sup>b</sup>	392 ± 10	
7.1 ± 0.1*	(9.8 ± 1.0) × 10 <sup>-4</sup> <sup>a</sup>	325 ± 10	7.2 ± 0.2*	(1.5 ± 0.5) × 10 <sup>-4</sup> <sup>a</sup>	299 ± 10	
8.5 ± 0.1	(1.0 ± 0.1) × 10 <sup>-4</sup> <sup>b</sup>	215 ± 10	8.4 ± 0.1	(8.9 ± 0.4) × 10 <sup>-5</sup> <sup>c</sup>	159 ± 10	

(a-c): the steady-state values were determined from the last a) 5, b) 6, c) 9 samplings.

\*: a concentration of (1.6 ± 0.6) × 10<sup>-3</sup> M was determined in a previous experiment in J-13 water at 25°C and pH 7.0.<sup>1</sup>

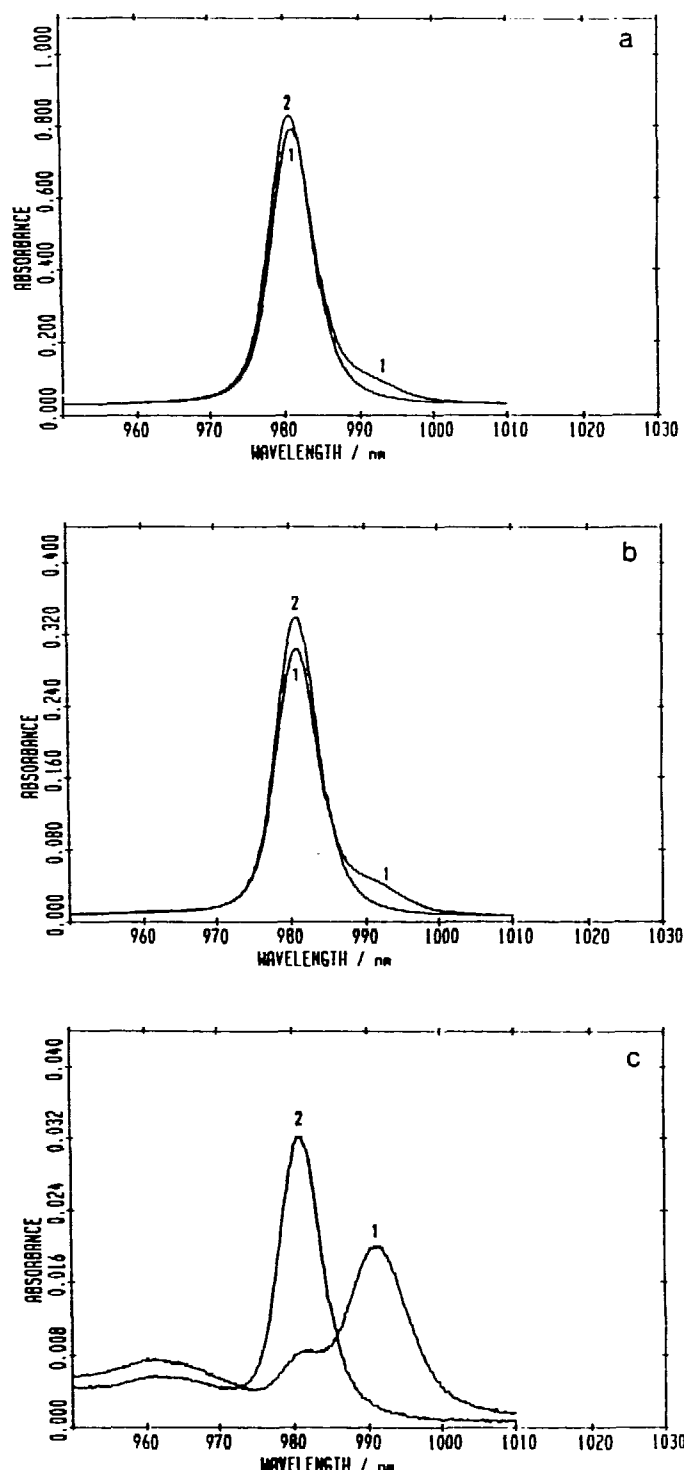


Figure 5. Near-IR absorption spectra of Np supermatant solutions at steady-state formed in J-13 groundwater at 60°C in (a) pH 5.9, (b) pH 7.1, (c) pH 8.5: (2) solution (1) acidified with  $\text{HClO}_4$  to pH 0.

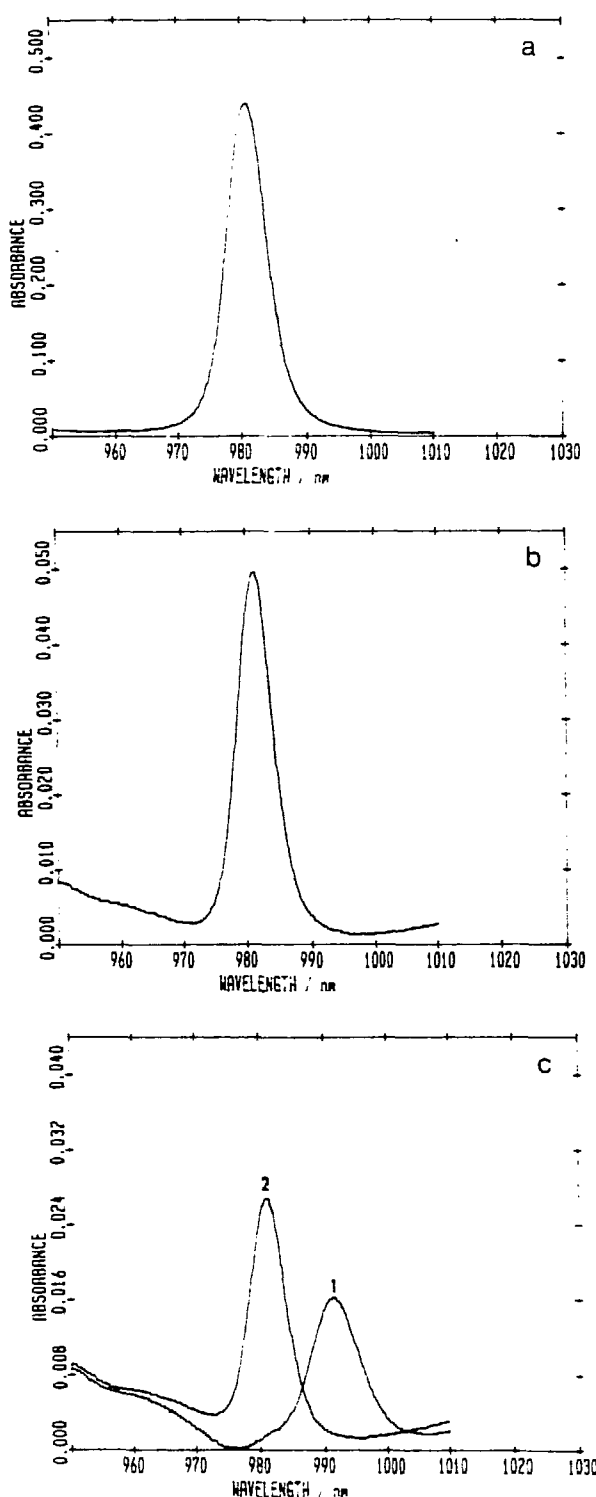


Figure 6. Near-IR absorption spectra of Np supermatant solutions at steady-state formed in J-13 groundwater at 90°C. (a) pH 5.9, (b) pH 7.2, (c) pH 8.4; (2) solution (1) acidified with  $\text{HClO}_4$  to pH 0.

After each solution was acidified with  $\text{HClO}_4$  to pH 0 the absorption spectra showed only the band at 980 nm. For the 90°C experiment, the pH 5.9 and pH 7.2 solution spectra show only the  $\text{NpO}_2^+$  main absorption band at 980 nm. The pH 8.4 solution, however, has the absorption band only at 992 nm where the characteristic neptunyl(V) carbonate band exists. After acidifying this solution with  $\text{HClO}_4$  to pH 0, the absorption band shifted back to 980 nm. These facts show increased carbonate complexation with increasing pH in the 60°C series, while only the pH 8.4 solution at 90°C contained carbonate complexes. The amount of carbonate complexing increased with temperature from 84 to 100% for the pH 8.5 solutions.

#### 5.2.1.3. Identification of Solids

The precipitates formed in the neptunium solutions were collected by centrifugation, washed with a small amount of  $\text{CO}_2$ -free water, and dried with an argon-jet. All precipitates at 60°C had a bright lime green color similar to the precipitate formed in the  $\text{NpO}_2^+$  solubility experiment in J-13 groundwater at pH 7 and 25°C, which was conducted for LANL during FY '84.<sup>1</sup> X-ray powder diffraction patterns taken from the precipitates produced distinct lines; d-spacings and relative intensities are listed in Table VI. The materials were crystalline; the individual patterns, however, were different from each other and no reference pattern could be found in the literature. To further identify the nature of these solids, the x-ray capillaries were viewed under a microscope. Color photographs of the view are shown for pH 5.9 in Figure 7 and for pH 7.1 and pH 8.5 in Figure 8. The photos show that the pH 5.9 precipitate contains two separate phases while the pH 7.1 and pH 8.5 precipitates contain only one phase. The solids at pH 7.1 and pH 8.5 appear microcrystalline and of an approximate size of 1 to 10  $\mu\text{m}$ . The pH 5.9 solid was made of bright-green flat shingles of up to 200  $\mu\text{m}$  which were interlayered by white spherical particles which were up to 250  $\mu\text{m}$  in size. Comparison of the aggregate's powder pattern with those of  $\text{NaClO}_4$ ,  $\text{Na}_2\text{CO}_3$ ,

**Table VI. X-ray powder diffraction patterns of Np solid phases in J-13 groundwater at 60°C, pH 5.9 (phase 1), pH 7.1 (phase 2), and pH 8.5 (phase 3).**

d(Å)	phase 1		phase 2		phase 3	
	I <sup>a</sup>	d(Å)	I <sup>a</sup>	d(Å)	I <sup>a</sup>	
		9.94	s	8.76	t	
7.30	t	7.50	t	7.95	t	
5.06	s	6.26	w-	6.66	m+	
4.80	m-	4.96	s	4.98	w+	
4.41	w+	4.33	s	4.75	s	
4.32	w-	4.03	vs	4.31	s	
4.05	vs	3.32	s	4.02	vs	
3.32	s	3.23	s	3.86	t	
3.21	w+	3.08	w+	3.60	t	
2.93	w-	2.70	m+	3.31	m+	
2.69	m+	2.55	s	3.19	s	
2.55	s	2.16	w-	2.87	w+	
2.40	t	2.06	w-	2.67	w-	
2.28	w+	2.02	w-	2.54	m-	
2.21	t	1.94	w-	2.37	t	
2.16	s	1.84	w+	2.27	t	
2.10	t	1.80	w+	2.15	m+	
2.02	w+	1.65	t	2.08	w-	
1.85	m-	1.49	w-	2.02	w-	
1.80	m-	1.47	t	1.97	t	
1.65	m-	1.45	t	1.89	t	
1.50	w-	1.41	t	1.84	t	
1.47	t			1.79	t	
				1.65	w+	
				1.50	t	

(a) Relative intensities visually estimated vs = very strong, s = strong, m = medium, w = weak, t = trace.

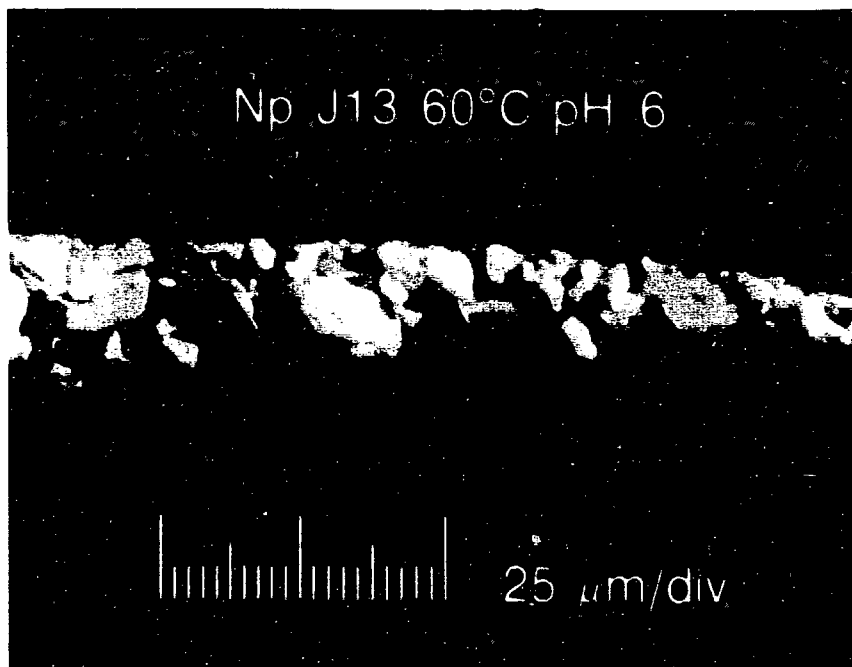


Figure 7. Microscopic view of  $^{237}\text{Np}$  solid obtained from supersaturation in J-13 groundwater at 60°C and pH 5.9. The solid is crystalline and contains carbonate. (BBC876-5178A).

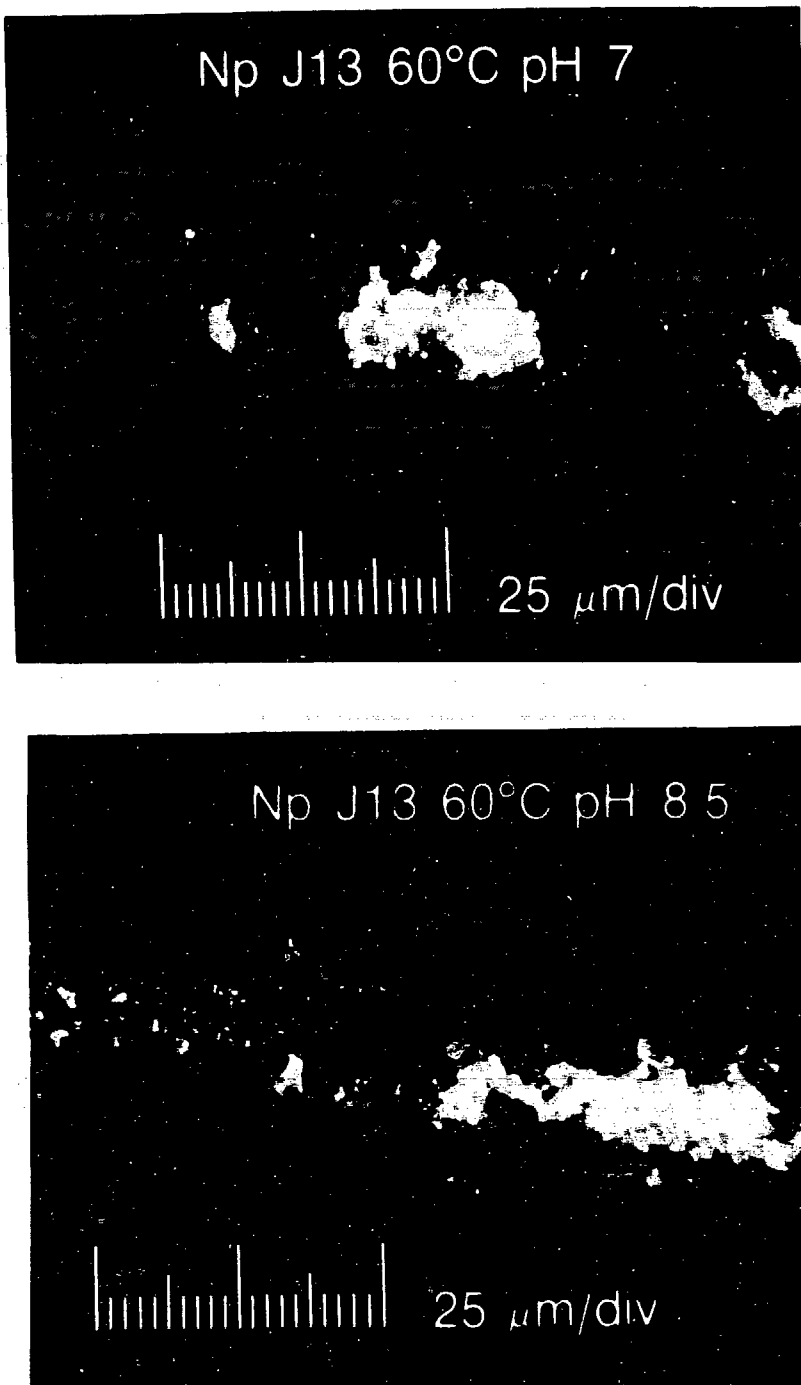


Figure 8. Microscopic view of  $^{237}\text{Np}$  solid obtained from supersaturation in J-13 groundwater at 60°C and (a) pH 7.1 (upper), (b) pH 8.5 (lower). The solids are crystalline and contain carbonate. (BBC876-5192A, BBC876-5194A).

$\text{NaHCO}_3$  (as possible non-actinide solid phases) proved the absence of such compounds.

The precipitates formed in the solutions at 90°C had the following colors:

pH 5.9 – dark brown to black

pH 7.2 – light brown

pH 8.4 – light green

From the solution at pH 8.4, two different precipitates were isolated by fractionated centrifugation, because the wet solid appeared to be composed of a tan and a green phase. When dried, these solids became identically light green. X-ray powder diffraction patterns taken from the precipitates produced distinct lines; the d-spacings and relative intensities of the crystalline materials are listed in Tables VII and VIII. The pH 5.9 solid was conclusively identified by matching its pattern with that of  $\text{Np}_2\text{O}_5$ .<sup>19</sup> Although the powder pattern of  $\text{Np}_3\text{O}_8$  is nearly identical to that of  $\text{Np}_2\text{O}_5$ , the former compound contains a 2:1 ratio of Np(V) to Np(VI). Spectrophotometry on the dissolved pH 5.9 precipitate established the absence of Np(VI), thereby identifying the solid formed as pure  $\text{Np}_2\text{O}_5$ . This phase was also present in the pH 7.2 precipitate together with another phase it had in common with the pH 8.4 precipitates; the x-ray diffraction lines are listed in Table VIII. The other phase corresponds well to the published pattern of  $\text{KNpO}_2\text{CO}_3$ . We exclude the existence of this compound in J-13 groundwater since the potassium content of this water is far lower than the sodium content.<sup>2</sup> The formation of an isostructural sodium analogue is more likely under these conditions. However, none of the published patterns of sodium neptunyl(V) carbonates with varying stoichiometry and hydration number can unequivocally provide a complete match for this phase.<sup>9-12</sup> From microscopic viewing of the 90°C solids contained in the x-ray capillaries (photographs are being taken currently), we confirmed that the solid formed at pH 7.2 was composed of multiple phases. Three phases were

**Table VII. X-ray powder diffraction patterns of Np solid phases in J-13 groundwater at 90°C, pH 5.9 (phase 1), and pH 7.2 (phase 2) compared with the pattern of  $\text{Np}_2\text{O}_5$ .<sup>19</sup>**

$\text{Np}_2\text{O}_5$		phase 1		phase 2	
d(Å)	I/I <sub>0</sub>	d(Å)	I <sup>a</sup>	d(Å)	I <sup>a</sup>
		8.85*	m	8.82*	s
		7.18*	m-	7.05*	m-
4.18	90	4.16	m+	4.19	m
				4.04	m
3.47	100	3.46	vs	3.46	vs
3.30	90	3.28	w+	3.30	m-
2.678	100	2.67	m+	2.67	s
2.666	100				
2.586	90	2.58	w	2.59	w-
		2.35	w-	2.55	w+
				2.27	w-
				2.15	w
2.092	60	2.09	w-	2.09	t
2.043	90	2.05	w+	2.05	t
				2.02	t
1.934	90	1.94	w+	1.94	w-
1.841	60	1.84*	w-	1.84	w+
1.831	60				
1.796	60	1.80	m-	1.80	w+
1.790	60				
1.766	40				
1.757	60	1.76*	m-	1.76*	w
1.754	60				
1.736	60	1.74	w+	1.74	w-
		1.70	t		
		1.65	t	1.64	w
1.616	40	1.61	m	1.61	w
1.607	40				
1.600	40			1.59	t
1.531	40	1.53	w-		
		1.51	t	1.50	w+
1.464	20	1.47	w		
1.456	20	1.43	m-		
1.421	20				
1.418	20				
1.396	20	1.40	t		
1.340	20	1.34*	m+	1.34	m-
1.333	20	1.30	w+	1.27	w-
1.334	20	1.29	w-		
		1.28	w		
		1.26	t		
		1.23	w		
		1.21	w-		
		1.19	t		
		1.16*	w		

(a) Relative intensities visually estimated: vs = very strong, s = strong, m = medium, w = weak, t = trace.

\* denotes diffuse bands

**Table VIII. X-ray powder diffraction patterns of Np solid phases in J-13 groundwater at 90°C, pH 7.2 (phase 2), and pH 8.4 (green: phase 3; tan: phase 4) compared with the pattern of KNpO<sub>2</sub>CO<sub>3</sub>.<sup>20</sup>**

	KNpO <sub>2</sub> CO <sub>3</sub>	phase 2		phase 3		phase 4		phase 4 (cont'd)	
		d(Å)	I <sup>a</sup>	d(Å)	I <sup>a</sup>	d(Å)	I <sup>a</sup>	d(Å)	I <sup>a</sup>
		8.82*	s	10.08	t	9.99	s-	1.84	m+
		7.05*	m-	8.59	w+	9.72	s	1.79	m
5.01	s	5.01	w-	7.00	w	8.63	w+	1.75	t
4.44	m	4.19	m	6.41	w-	8.37	m	1.65	m+
4.06	vs	4.04	m	5.04	m-	4.99	s	1.59	w
		3.46	vs	4.65	t	4.90	w+	1.57	w-
3.31	s	3.30	m-	4.43	m	4.64*	w	1.49	m
2.66	m	2.67	s	4.23	w-	4.41	m+	1.47	w+
2.56	m	2.59	w-	4.05	vs	4.23	m-	1.42	w
2.49	m	2.55	w+	3.34	w+	4.04*	vs	1.40	t
2.28	m	2.27	w-	2.68	w-	3.66*	w	1.37	t
2.22	w	2.15	w	2.55	m	3.50	t	1.34	w-
2.16	s	2.09	t	2.28	w-	3.32	s	1.29	w
		2.05	t	2.16	w	3.20	w+	1.28	w+
2.02	m	2.02	t	2.03	w-	3.12	w-	1.24	w-
		1.94	w-	1.84	w	3.04	t	1.22	w
1.85	m-	1.84	w+	1.80	w	2.91	w	1.15	w-
1.82	m	1.80	w+	1.65	w+	2.81	t	1.14	w
1.79	m	1.76*	w	1.49	w	2.77	t		
		1.74	w-	1.22	t	2.67	m-		
1.65	m+	1.64	w	1.19	t	2.55	s		
		1.61	w			2.51	m-		
1.59	w	1.59	t			2.46	w-		
1.56	w-	1.50	w+			2.27	m		
1.50	w	1.34	m-			2.21	w		
1.48	w-	1.27	w-			2.16	m+		
						2.12	w		
						2.02	m-		
						1.99	t		
						1.96	t		

(a) Relative intensities visually estimated: vs = very strong, s = strong, m = medium, w = weak, t = trace.

\* denotes diffuse bands

distinguishable: the major phase was light brown and finely crystalline, another one was dark brown and coarsely crystalline, and a minor phase was bright green colored.

To gain additional information on the nature of the neptunium precipitates, we treated a small portion of each with 1 M  $\text{HClO}_4$  to test for the presence of carbonate. This test is positive if the solid dissolves with the evolution of gas, which is very likely  $\text{CO}_2$ . The 60°C solids increased gas evolution with increasing pH. This may indicate increasing carbonate content, but the varying crystallite size may also influence the rate of gas release. Near-IR spectrophotometry of the dissolved solids showed the neptunium present in the +5 state, assuming that no change in oxidation state occurred during the dissolution. We used spark emission spectroscopy of the dissolved precipitates to determine their composition in more detail. The results, given in Table IX, indicate the virtual absence of expected alkali metal and alkaline earth ions which would be found if the solids were composed of  $\text{Na}_3\text{NpO}_2(\text{CO}_3)_2$ ,  $\text{CaNaNpO}_2(\text{CO}_3)_2$ , or  $\text{MgNaNpO}_2(\text{CO}_3)_2$ . We attempted to verify of this rather surprising result by submitting these samples to Los Alamos National Laboratory (LANL) for NAA. If the samples are returned within the time frame of our J-13 investigations, we will analyze them by FTIR.

We also tested the 90°C solids for carbonate. The pH 5.9 precipitate dissolved sparingly with no detectable gas evolution, as was expected of  $\text{Np}_2\text{O}_5$ . The pH 7.2 solid released some gas, and the pH 8.4 precipitate produced significant amounts of gas; both solids dissolved completely. The findings that the pH 7.2 and pH 8.4 solids contained carbonate are supported by their FTIR spectra given in Figures 9, 10, and 11. In particular the characteristic C-O stretching bands between approximately 1300 and 1500  $\text{cm}^{-1}$  indicate the presence of coordinated carbonate in the pH 7.2 and pH 8.4 solids.<sup>13</sup> The pH 5.9 solid is too opaque to obtain an interpretable transmission spectrum in this wavelength region, as shown in Figure 12. Furthermore, the absorptions in all three FTIR spectra at approximately 830  $\text{cm}^{-1}$  are characteristic of the

**Table IX. Spectrochemical analyses of the Np solid phases in J-13 groundwater at 60°C and pH 5.91, pH 7.01, and pH 8.48.**

pH of sol.	Np	Na	Ca	Mg	K	Si	Fe
5.91	100	<1	0.2	0.2	<1	≤0.01	<0.01
7.01	100	<1	0.5	0.3	<1	≤0.01	<0.01
8.48	100	<1	2.0	0.5	<1	≤0.01	<0.01

Numbers represent weight percent.

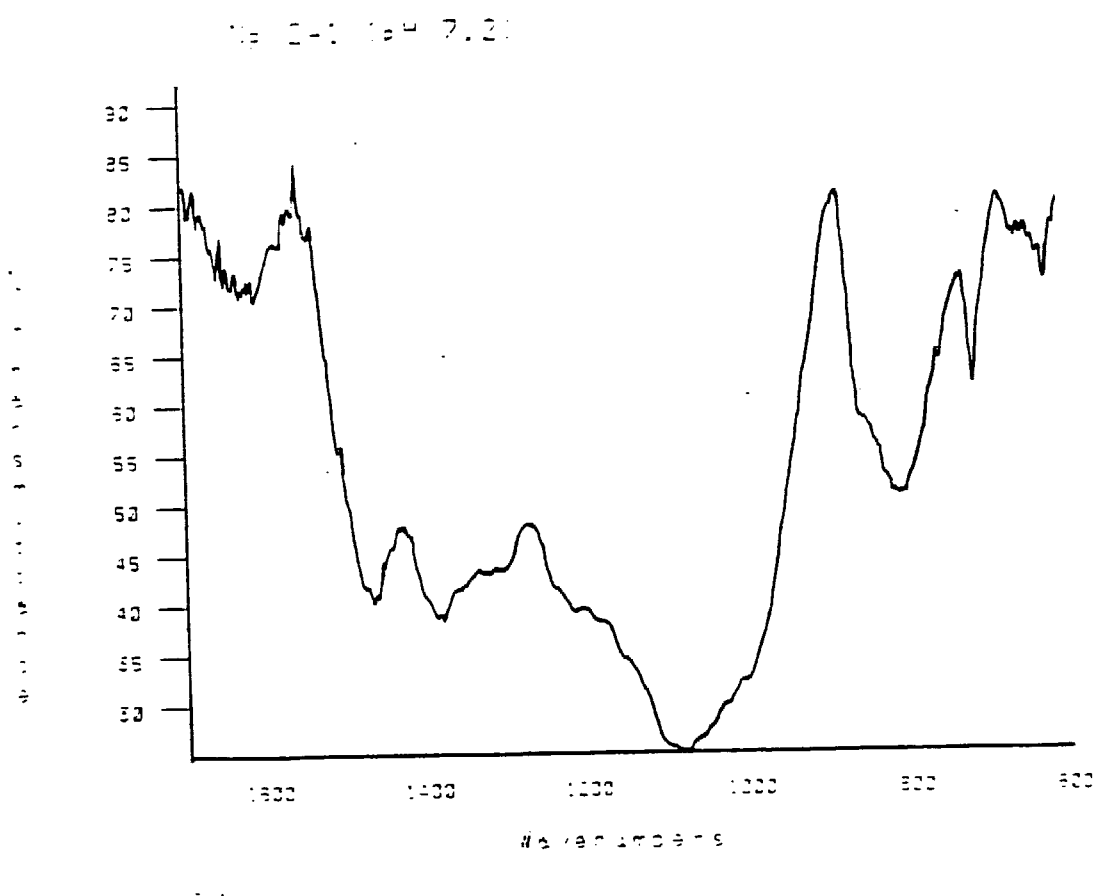


Figure 9. FTIR spectrum of Np solid phase formed at pH 7.2 and 90°C in J-13 groundwater.

REPRODUCED FROM BEST  
AVAILABLE COPY

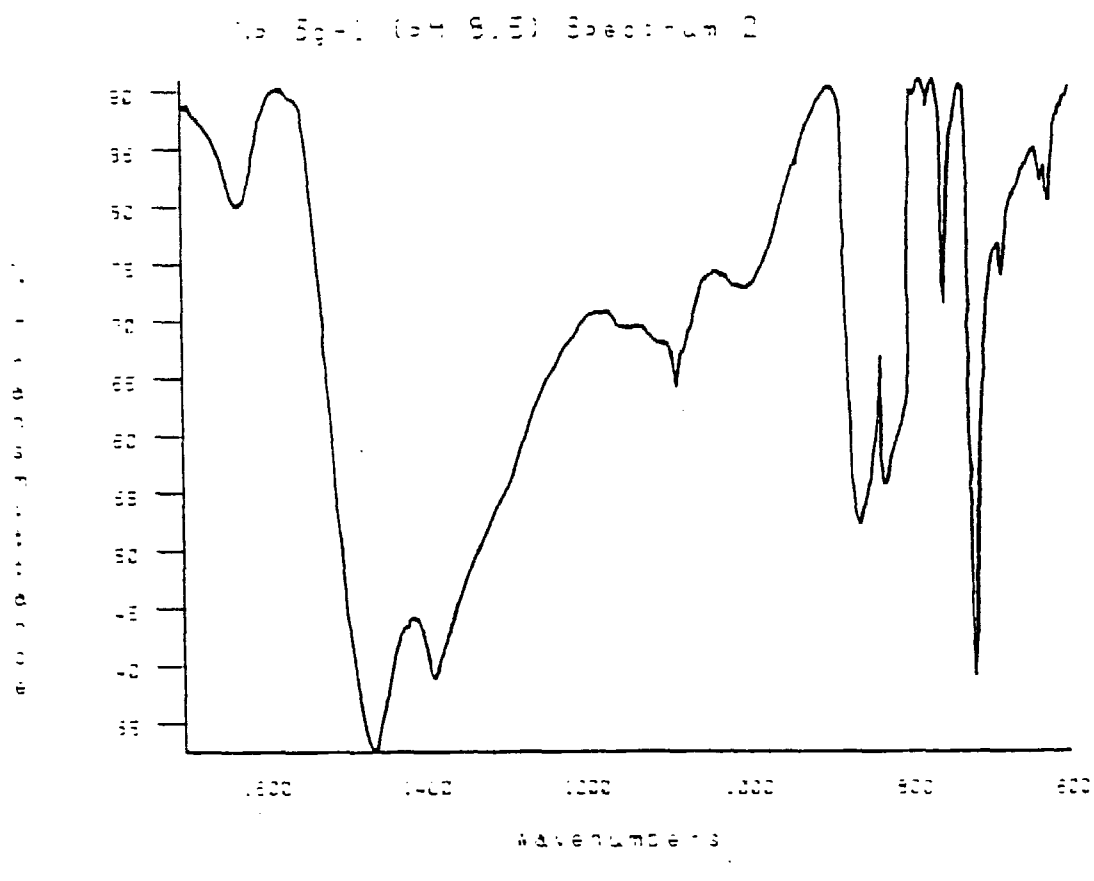


Figure 10. FTIR spectrum of Np solid (green phase) formed at pH 8.4 and 90°C in J-13 groundwater.

REPRODUCED FROM BEST  
AVAILABLE COPY

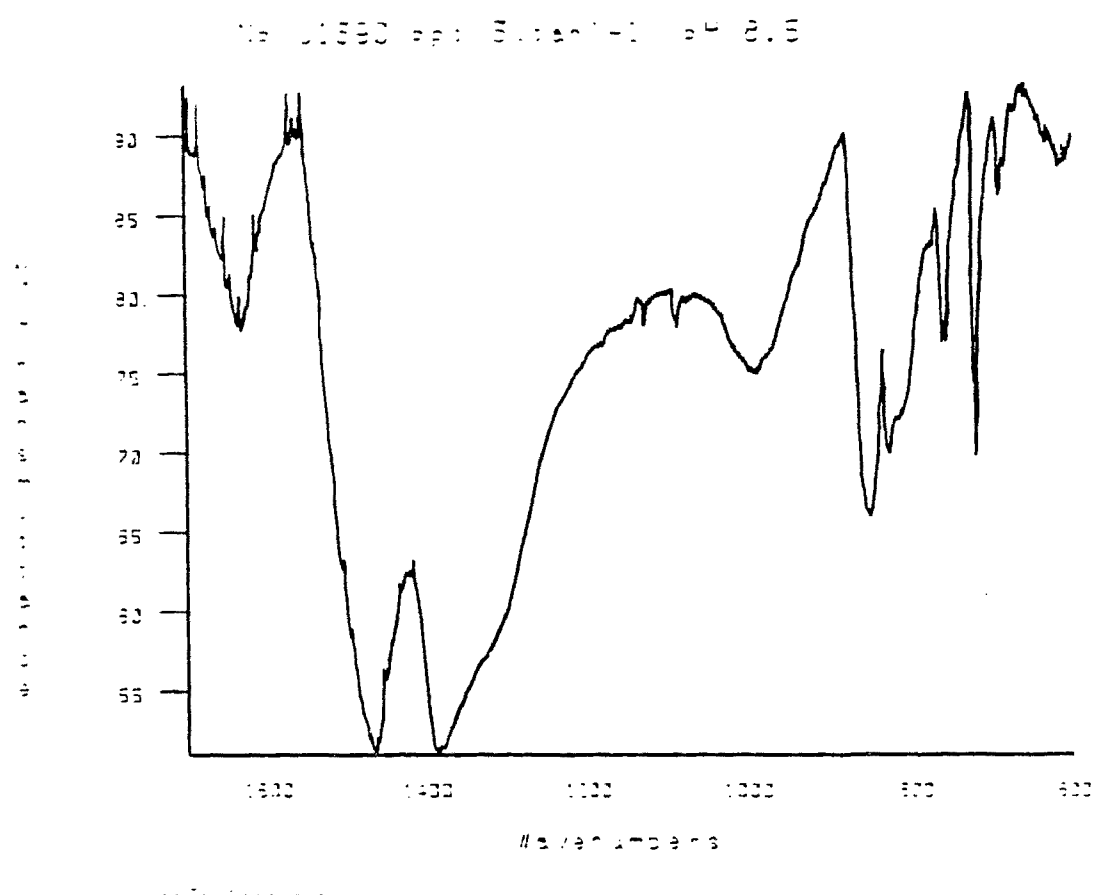


Figure 11. FTIR spectrum of Np solid (tan phase) formed at pH 8.4 and 90°C in J-13 groundwater.

REPRODUCED FROM BEST  
AVAILABLE COPY

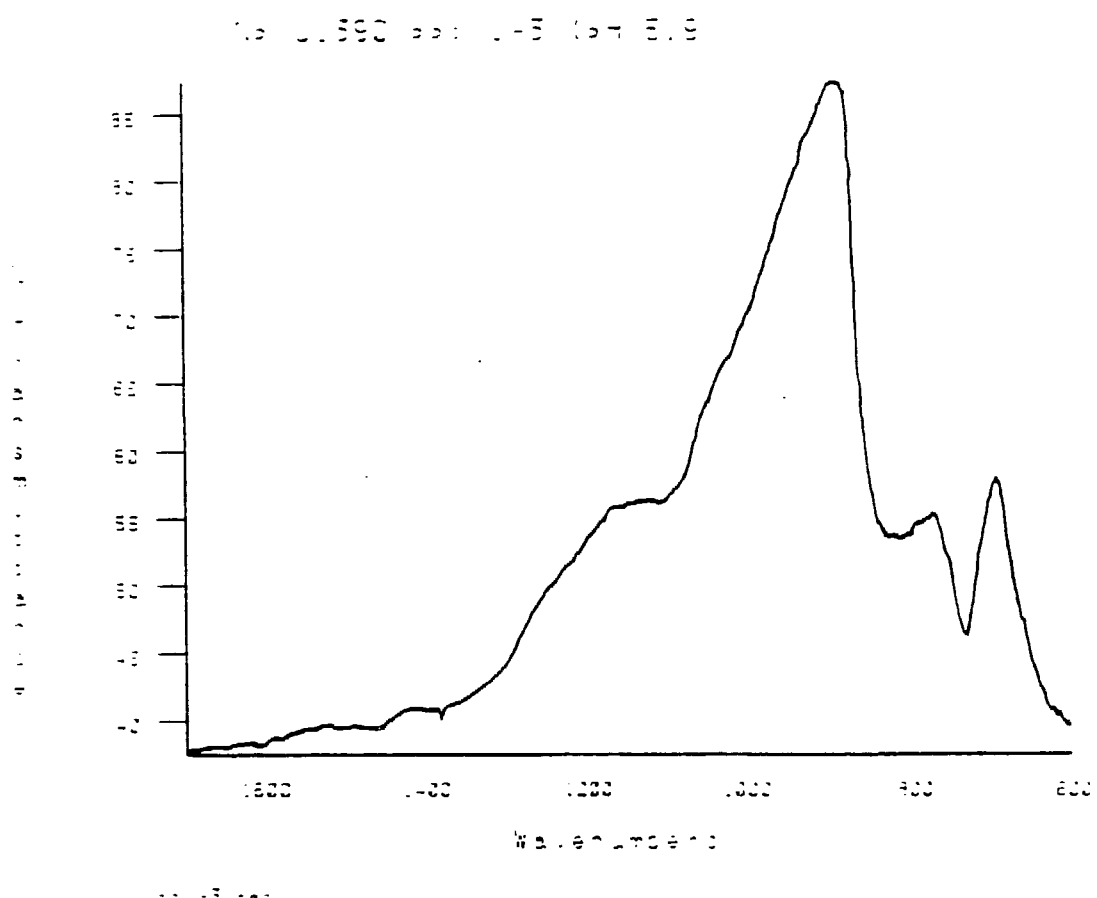


Figure 12. FTIR spectrum of Np solid phase formed at pH 5.9 and 90°C in J-13 groundwater.

REPRODUCED FROM BEST  
AVAILABLE COPY

asymmetric neptunyl(V) stretch, which proves that the neptunium remained pentavalent in solid phases.<sup>14</sup> This is also supported by the electronic near-IR spectra of the dissolved solids. The only feature observed in these spectra is the 980 nm absorption, characteristic of  $\text{NpO}_2^+$ .

In summary, except for the 90°C experiment at pH 5.9, the data from these different characterization methods do not unambiguously identify the neptunium solid phases. The NAA, already initiated for the 60°C solids and planned for the 90°C solids, should further clarify their nature.

### 5.2.2. Plutonium

#### 5.2.2.1. Solubility

The results of the solubility measurements as a function of equilibration time and pH for 60° and 90°C are given in Figures 13 and 14, respectively. Steady-state concentrations and the solutions' Eh values are given in Table X. The steady-state concentrations decrease with increasing temperature at all three pH values investigated. A third measurement taken previously in J-13 water at pH 7 and 25°C, further supports this trend.<sup>1</sup> Furthermore, the concentrations of the 60°C experiments increase with increasing pH, while they remain nearly constant for the 90°C series.

#### 5.2.2.2. Oxidation State Determination

The plutonium supernatant solutions at steady state were analyzed for their oxidation state distributions. The speciation studies are made difficult by the low solubility of plutonium. The solutions' concentration levels lie below the sensitivity range of methods such as absorption spectrophotometry, which would allow the direct measurement of the species present. Therefore, a scheme was developed to determine the oxidation states indirectly. The method involves a combination of solvent extractions and coprecipitation. It was tested on solutions of known plutonium oxidation state

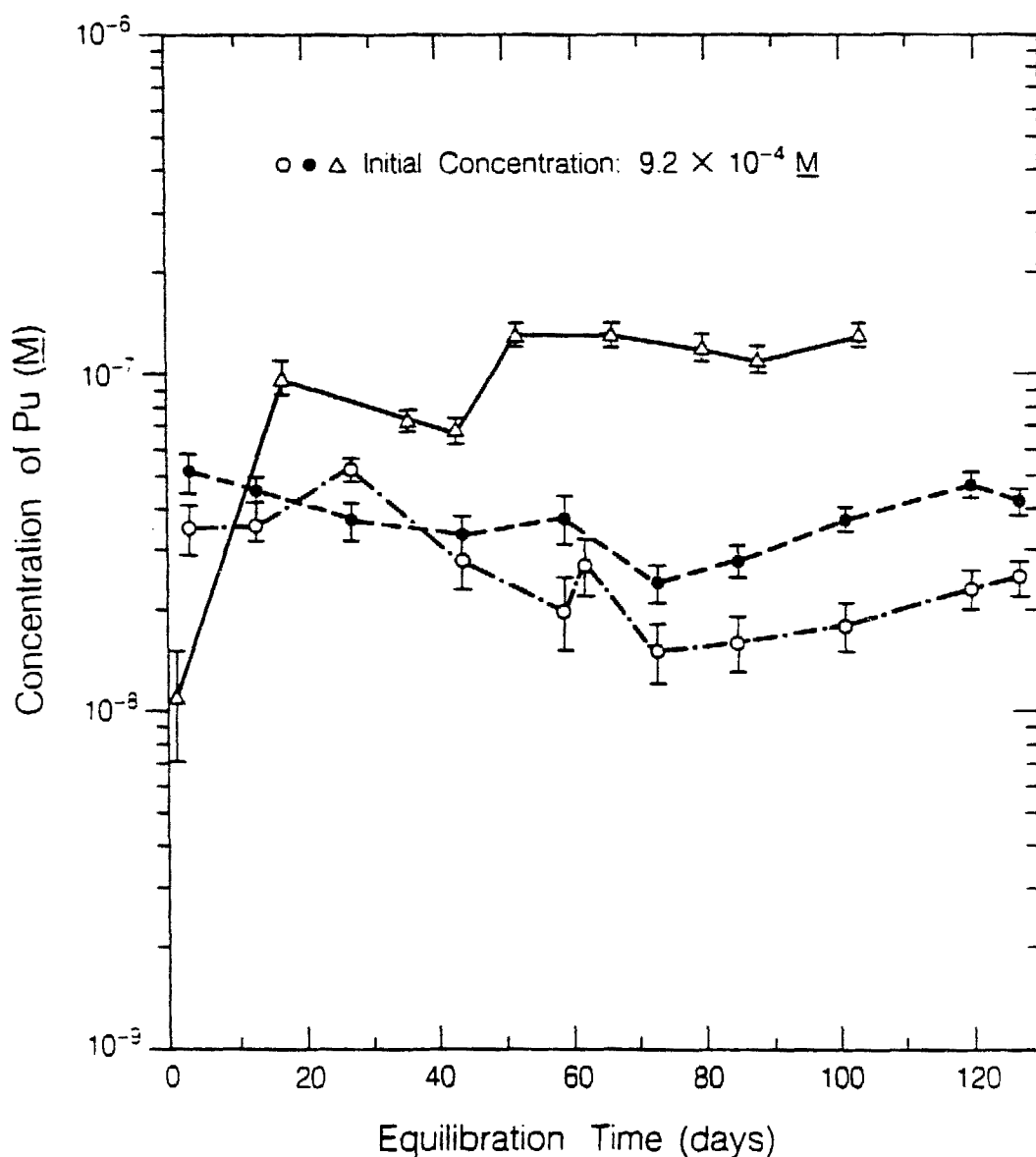


Figure 13. Solution concentrations of  $^{239}\text{Pu}$  in contact with precipitate obtained from supersaturation in J-13 groundwater at 60°C as a function of time. pH 5.9  $\pm$  0.1 (open circles), pH 7.0  $\pm$  0.1 (filled circles), and pH 8.5  $\pm$  0.1 (triangles). The plutonium was added initially (day 0) as  $\text{Pu}^{3+}$ .

Approach of J-13 Water Solutions of Pu  
to Equilibrium at 90 Degrees C

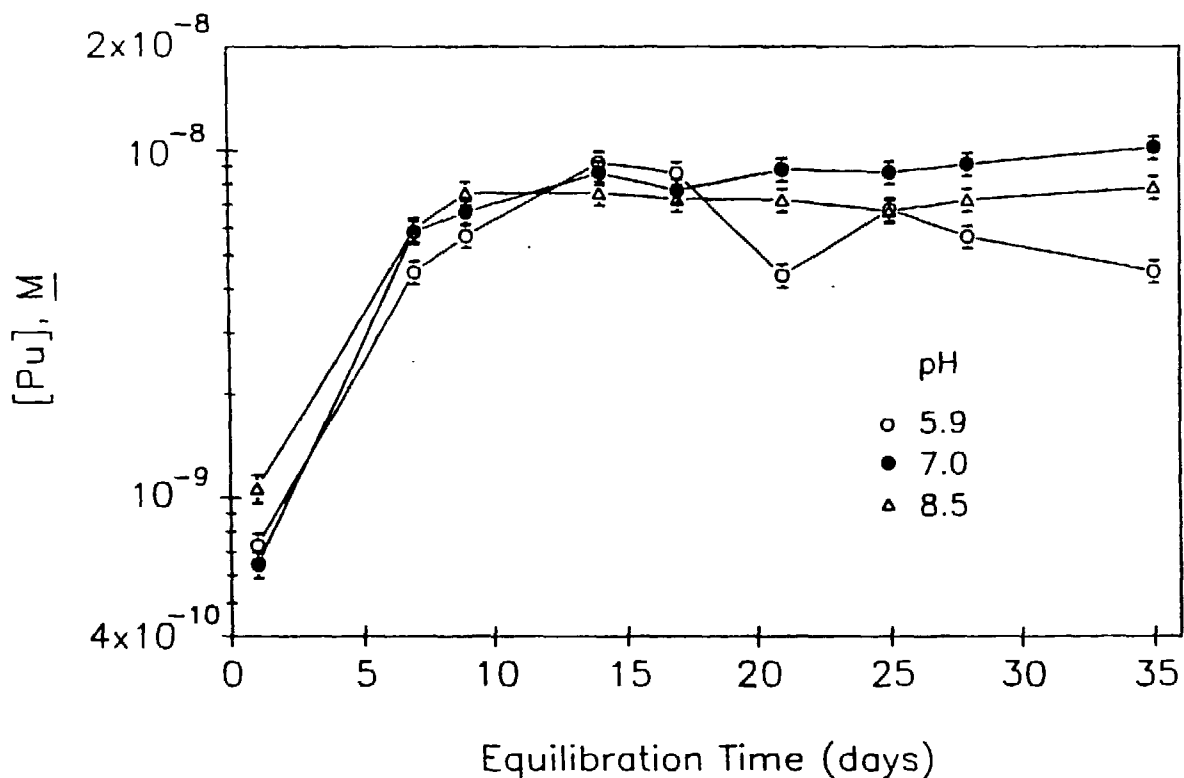


Figure 14. Solution concentration of  $^{239}\text{Pu}$  in contact with precipitate obtained from supersaturation in J-13 groundwater at 90°C as a function of time. pH 5.9  $\pm 0.3$  (open circles), pH 7.2  $\pm 0.2$  (filled circles), and pH 8.5  $\pm 0.1$  (triangles). The plutonium was added initially (day 0) as  $\text{Pu}^{4+}$  at initial concentrations of  $6.3 \times 10^{-4}$  M.

**Table X. Comparison of steady-state solution concentrations for Pu in J-13 groundwater at 60°C and 90°C.**

Pu	60°C			90°C		
	pH	conc. (M)	Eh (mV vs. NHE)	pH	conc. (M)	Eh (mV vs. NHE)
5.9 ± 0.1	(2.7 ± 1.7) × 10 <sup>-8<sup>a</sup></sup>	451 ± 10	5.9 ± 0.3	(6.2 ± 1.9) × 10 <sup>-9<sup>c</sup></sup>	360 ± 10	
7.0 ± 0.1 <sup>a</sup>	(3.8 ± 0.8) × 10 <sup>-8<sup>a</sup></sup>	386 ± 10	7.2 ± 0.2 <sup>a</sup>	(8.8 ± 0.8) × 10 <sup>-9<sup>d</sup></sup>	376 ± 10	
8.5 ± 0.1	(1.2 ± 0.1) × 10 <sup>-7<sup>b</sup></sup>	241 ± 10	8.5 ± 0.1	(7.3 ± 0.4) × 10 <sup>-9<sup>d</sup></sup>	133 ± 10	

(a-e) : The steady-state values were determined from (a) all, the last (b) 5, (c) 8, (d) 6, samplings.

<sup>a</sup> : a concentration of (1.6 ± 0.2) × 10<sup>-6</sup> M was determined in a previous experiment in J-13 water at 25°C and pH 7.0.<sup>1</sup>

mixtures with both high-level and trace-level concentrations. We issued a report describing the details of this method.<sup>15</sup>

Results of this study for 60° and 90°C are given in Table XI. At 60°C the solutions contained predominantly Pu(V) and Pu(VI); as the amount of Pu(V) increases with pH, the Pu(VI) decreases. At 90°C, however, only small quantities of Pu(VI) are present, while large amounts of Pu(V) coexist with smaller amounts of Pu(IV), Pu(III), and Pu(IV) polymer. At pH 7, Pu(V) is measured to be equal to the sum of Pu(III) and Pu(IV) polymer. We explain this measured decrease of Pu(V) and the increase of Pu(III + poly.) by leakage of the Amicon filter used for phase separation. Such leakage would introduce more polymer and change the relative oxidation state distribution. This explanation is supported by comparison of the assay taken as a reference standard for the extraction at pH 7 and 90°C with the most recent sampling for the solubility determination; the extraction sample contained 2.36 times more plutonium. Unfortunately, we could not repeat this experiment, because not enough supernatant was left for the test.

In Table XII, the pH 7 oxidation state distributions for 60° and 90°C are also compared with those from a previous experiment at 25°C.<sup>1</sup> Pu(V) and Pu(VI) dominate the solutions of 25° and 60°C, while Pu(III), Pu(IV), and Pu(IV) polymer are present in insignificant quantities. The 90°C distributions are not directly comparable to the 25° and 60°C data for reasons already discussed.

### 5.2.2.3. Identification of Solids

The green plutonium precipitates found in the solutions at 60°C were collected by centrifugation, washed with a small amount of CO<sub>2</sub>- free water, and dried with an Ar-jet. D-spacings and relative intensities of the x-ray powder diffraction patterns from the precipitates are listed in Table XIII. As these patterns show, all three phases have several diffuse lines in common, but we found no reference pattern in the literature to

**Table XI. Distribution of Pu oxidation states in J-13 groundwater solutions at steady-state and various pH values and temperatures of 60° and 90°C.**

pH	Oxidation States (%)							
	Pu(IV)		Pu(V)		Pu(VI)		Pu(III + poly.)	
	60°C	90°C	60°C	90°C	60°C	90°C	60°C	90°C
5.9 <sup>a</sup>	2 ± 1	6 ± 5	17 ± 5	79 ± 7	72 ± 5	7 ± 5	10 ± 2	9 ± 5
7.0 <sup>b</sup>	2 ± 1	13 ± 1	44 ± 9	48 ± 3	52 ± 4	0 ± 6	3 ± 1	45 ± 2
8.5 <sup>c</sup>	13 ± 1	10 ± 2	58 ± 2	85 ± 4	24 ± 1	0 ± 6	5 ± 4	11 ± 2

poly. = Pu(IV) polymer

<sup>a</sup> 60°C: 5.9 ± 0.1; 90°C: 5.9 ± 0.3

<sup>b</sup> 60°C: 7.0 ± 0.1; 90°C: 7.2 ± 0.2

<sup>c</sup> 60°C: 8.5 ± 0.1; 90°C: 8.5 ± 0.1

**Table XII. Temperature effect on Pu oxidation state distribution in J-13 groundwater at pH 7 and various temperatures.**

Temp. (°C)	Oxidation States (%)			
	Pu(IV)	Pu(V)	Pu(VI)	Pu(III + poly.)
25	1 ± 1	39 ± 4	59 ± 2	1 ± 1
60	2 ± 1	44 ± 9	52 ± 4	3 ± 1
90	13 ± 1	48 ± 3	0 ± 6	45 ± 2

steady-state concentrations:

at 25°C,  $(1.6 \pm 0.2) \times 10^{-6}$  M

at 60°C,  $(3.8 \pm 0.8) \times 10^{-8}$  M

at 90°C,  $(8.8 \pm 0.8) \times 10^{-9}$  M

poly. = Pu(IV) polymer

**Table XIII. X-ray powder diffraction patterns of Pu solid phases in J-13 groundwater at 60°C, pH 5.9 (phase 1), pH 7.0 (phase 2), and pH 8.5 (phase 3).**

phase 1		phase 2		phase 3	
d(Å)	I <sup>a</sup>	d(Å)	I <sup>a</sup>	d(Å)	I <sup>a</sup>
		18.4*	w-		
10.5*	m				
6.43*	w+				
4.20*	s	4.20*	s	4.17*	vs
3.15*	t			3.03*	m
				2.41*	t
1.99*	vs	1.98	vs	1.99*	vs
1.75*	t	1.73*	w+	1.73*	w+

(a) Relative intensities visually estimated: vs = very strong, s = strong, m = medium, w = weak, t = trace.

\* denotes diffuse bands

assign the lines.

We tested the plutonium precipitates formed at 60°C for carbonate. When treated with 1 M HCl, each precipitate dissolved partially with the evolution of gas. The amount of gas evolution increased from the pH 5.92 to the pH 8.47 precipitate. The remaining precipitates were dissolved further with 6 M HCl/NaF, filtered through 220 nm pore size filters, and analyzed by absorption spectrophotometry. The spectra showed the characteristic absorption bands for Pu(IV) polymer. The presence of carbonate in these solids can be explained in several ways. Pu(IV) polymer absorbs CO<sub>2</sub> which converts on the polymer surface to carbonate.<sup>16</sup> The identification of the 60°C precipitates as Pu(IV) polymer is not confirmed by the x-ray data, since aged Pu(IV) polymer yields a pattern with diffuse lines at the same spacings as PuO<sub>2</sub>. In spite of the x-ray data, the sparing solubility in 6 M HCl and the need to use a NaF catalyst identify at least one component of the precipitate as Pu(IV) polymer. Another component could be a plutonium carbonate which would also test positive for carbonate. To further elucidate this matter, microscopic photographs of the solids contained in the x-ray capillaries were taken. The photos, shown in Figure 15 and 16, provide no evidence for multicomponent solids. To better identify these solids, samples we submitted to LANL for elemental analysis by NAA. We intend to take FTIR spectra upon their return.

The x-ray powder diffraction results for the plutonium precipitates formed at 90° C are listed in Table XIV. Most of the few lines observed were rather diffuse, indicating at most a low degree of crystallinity. We found no matching patterns in the literature. Close microscopic examination of the solids revealed at least two phases for the pH 5.9 precipitate. A yellow-green powdery phase, probably non-crystalline, was mixed with a smaller fraction of darker green clumps. Such a combination of crystalline and amorphous materials in this solid can explain the observed powder pattern which is composed of both very sharp and diffuse lines. The pH 7.2 solid was a

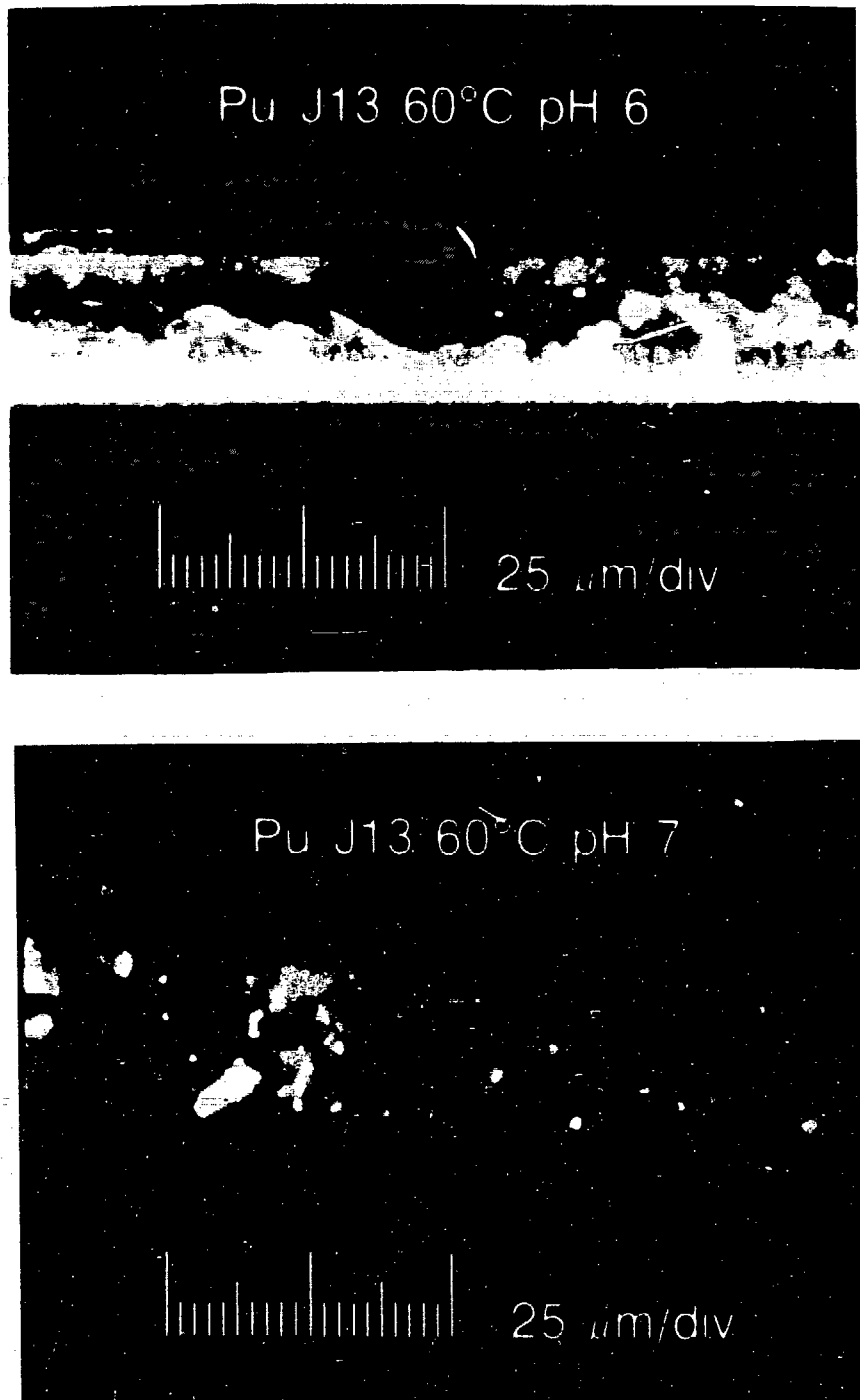


Figure 15. Microscopic views of  $^{239}\text{Pu}$  solids obtained from supersaturation in J-13 groundwater at 60°C and (a) pH 5.9 (upper), (b) pH 7.0 (lower). The solids contain carbonate. (BBC876-5176A, BBC876-5196A).

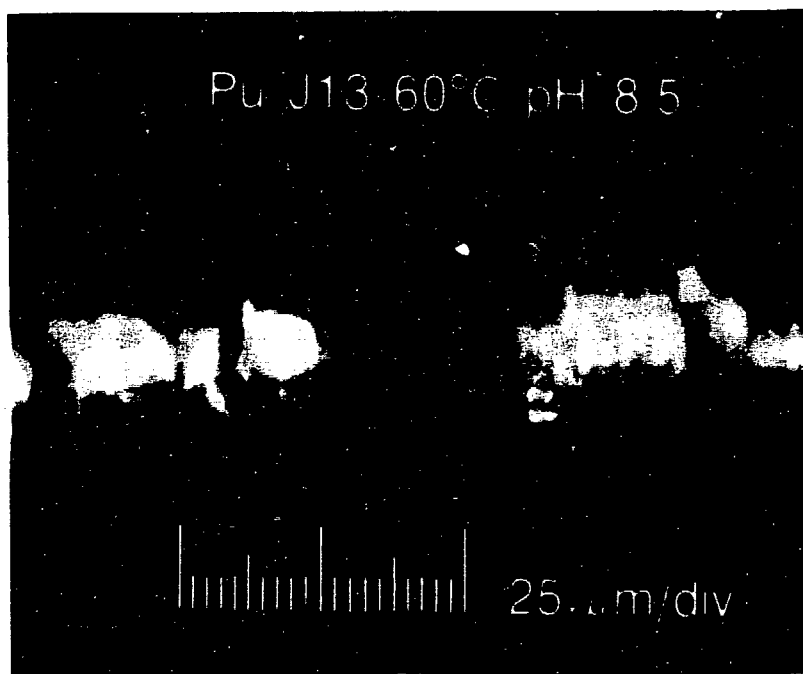


Figure 16. Microscopic view of  $^{239}\text{Pu}$  solids obtained from supersaturation in J-13 groundwater at 60°C and pH 8.5. The solids contain carbonate. (BBC876-5200A).

**Table XIV. X-ray powder diffraction patterns of Pu solid phases in J-13 groundwater at 90°C, pH 5.9 (phase 1), pH 7.2 (phase 2), and pH 8.5 (phase 3).**

phase 1		phase 2		phase 3	
d(Å)	I <sup>a</sup>	d(Å)	I <sup>a</sup>	d(Å)	I <sup>a</sup>
6.61*	s-	10.6*	s	10.1*	s
4.15*	vs	6.58*	m	4.17*	w+
3.15*	m	4.13*	m		
2.34	vs			1.92*	t
2.03	s				
1.94*	s			1.62*	t
1.90*	w				
1.70*	vs				
1.64*	w				
1.40	w+				
1.18	m-				

(a) Relative intensities visually estimated: vs = very strong, s = strong, m = medium, w = weak, t = trace.

\* denotes diffuse bands

yellow-green powder similar to the major phase at pH 5.9. The precipitate formed at pH 8.5 was a mixture of a similar-appearing yellow-green powder in which some lighter green pellets were embedded. The low crystallinity and the dominant yellow-green color of all three precipitates suggest that the solids consist mainly of polymeric Pu(IV). Further characterization of these solids was accomplished by FTIR spectroscopy; the spectra are depicted in Figures 17, 18, and 19. All three spectra show absorptions that can be assigned to carbonate-containing aged Pu(IV) polymer.<sup>16</sup> The split bands between 1350  $\text{cm}^{-1}$  and 1650  $\text{cm}^{-1}$  are characteristic of coordinated  $\text{CO}_3^{2-}$  ( $\nu_3$ ). The absorption(s) between 1000  $\text{cm}^{-1}$  and 1100  $\text{cm}^{-1}$  is correlated to aged Pu(IV) polymer. The sharp band at 625  $\text{cm}^{-1}$  is not characteristic of Pu(IV) polymer but remains unassigned. Elemental analyses of these precipitates are planned.

### 5.2.3. Americium

#### 5.2.3.1. Solubility

The results of the americium solubility experiment at 60°C are shown in Figure 20. Marked variations in the americium concentrations of each solution are evident from these data. No steady state was observed within the 168 days of the experiment. This behavior may be explained by an observation made at the end of each experiment. After removal of both solid and solution phases from the experimental cells, we noted marked pitting of the inner surfaces of the PTFE containers where particulate americium had adhered. Such pitting was not present in the  $^{237}\text{Np}$  or  $^{239}\text{Pu}$  experiments. We believe that this pitting is radiation damage from the  $\alpha$ -decay of  $^{243}\text{Am}$ . The PTFE particles dislodged by the radiation were not visible and are probably quite small. Such small particles may serve as adsorption sites for dissolved americium species, thus forming pseudocolloids. The irreproducible behavior of americium pseudocolloids in aqueous solution has been reported previously and may be responsible for the observed changes in concentration.<sup>18</sup> Future work at 90°C will be directed

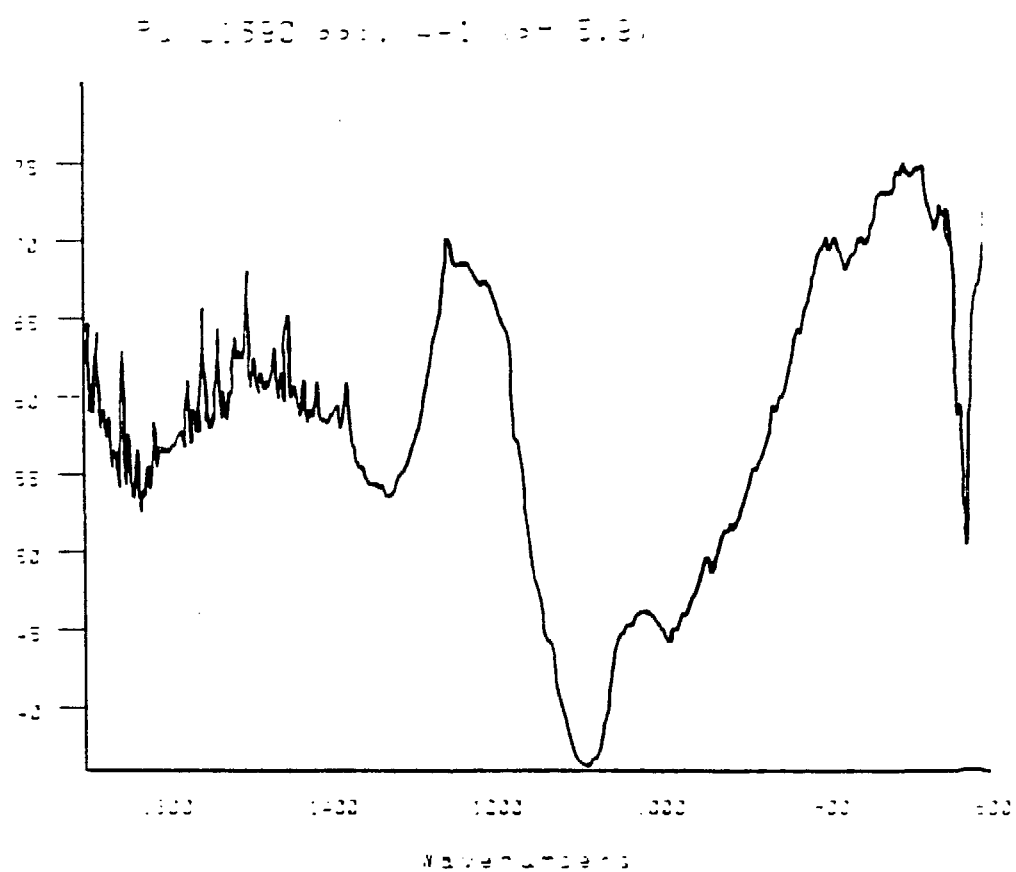


Figure 17. FTIR spectrum of Pu solid phase formed at pH 5.9 and 90°C in J-13 groundwater.

REPRODUCED FROM BEST  
AVAILABLE COPY

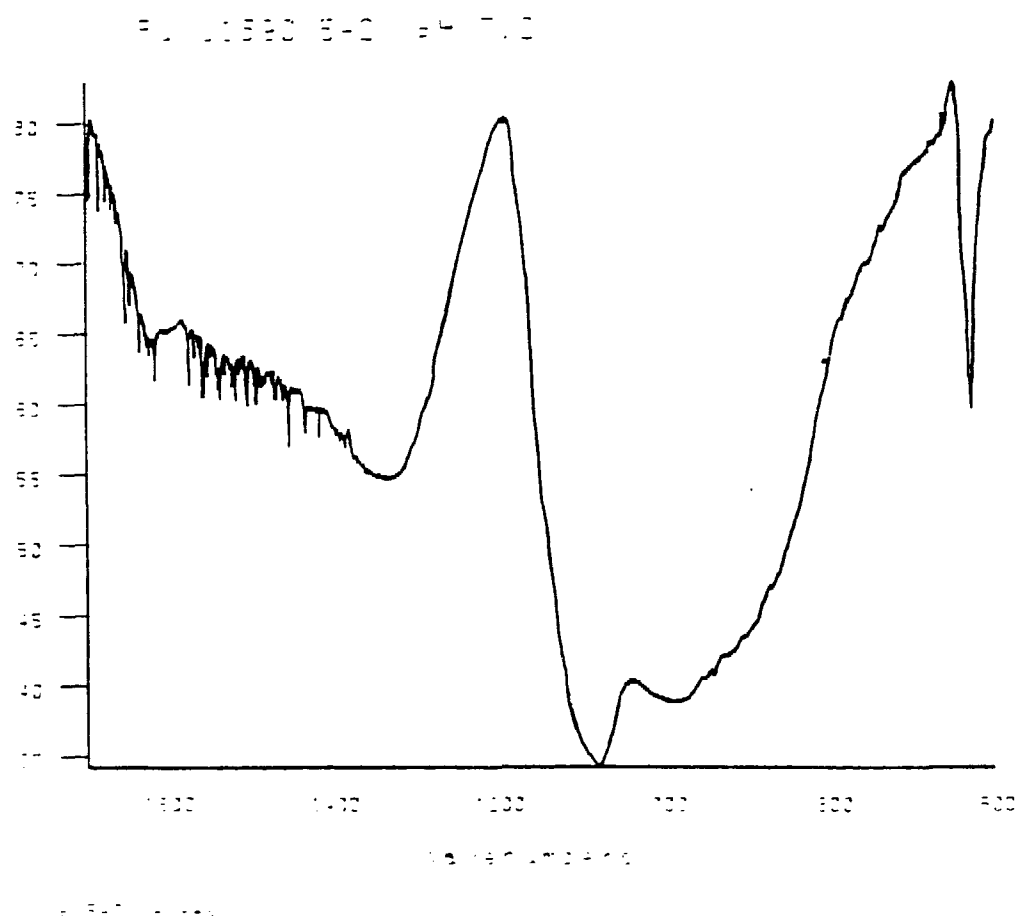


Figure 18. FTIR spectrum of Pu solid phase formed at pH 7.2 and 90°C in J-13 groundwater.

REPRODUCED FROM BEST  
AVAILABLE COPY

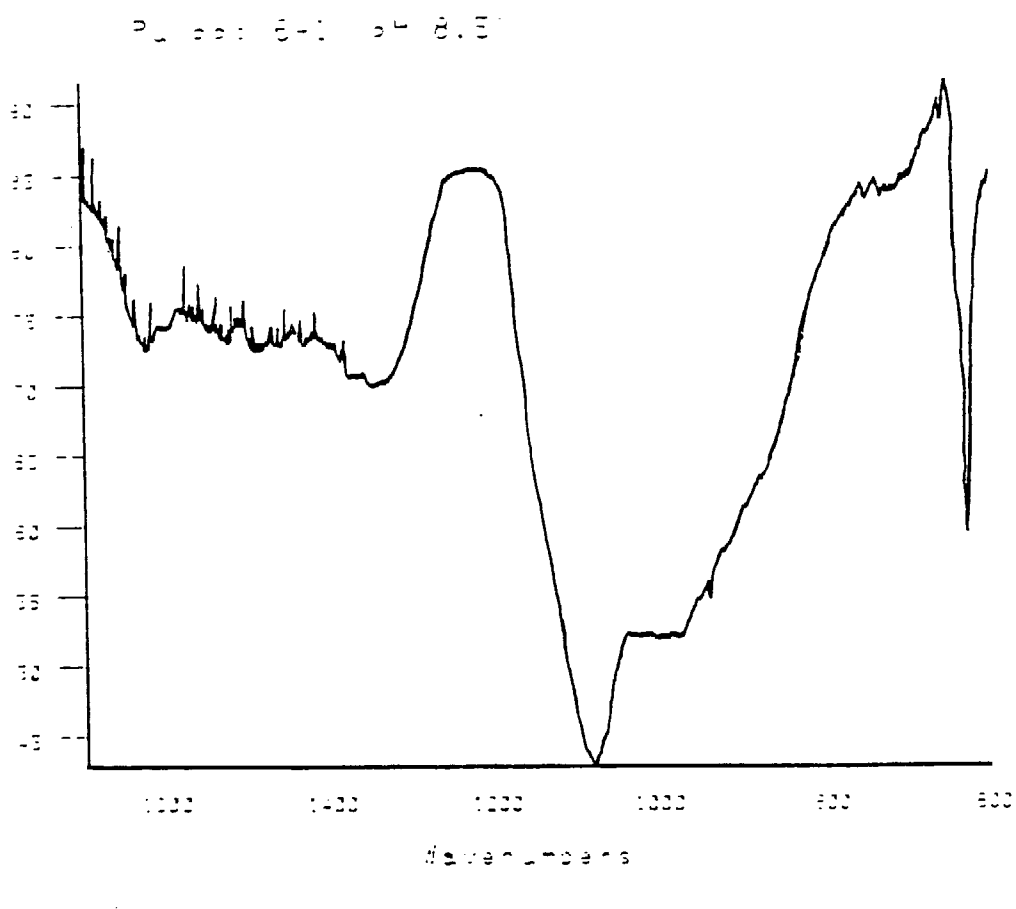


Figure 19. FTIR spectrum of Pu solid phase formed at pH 8.5 and 90°C in J-13 groundwater.

REPRODUCED FROM BEST  
AVAILABLE COPY

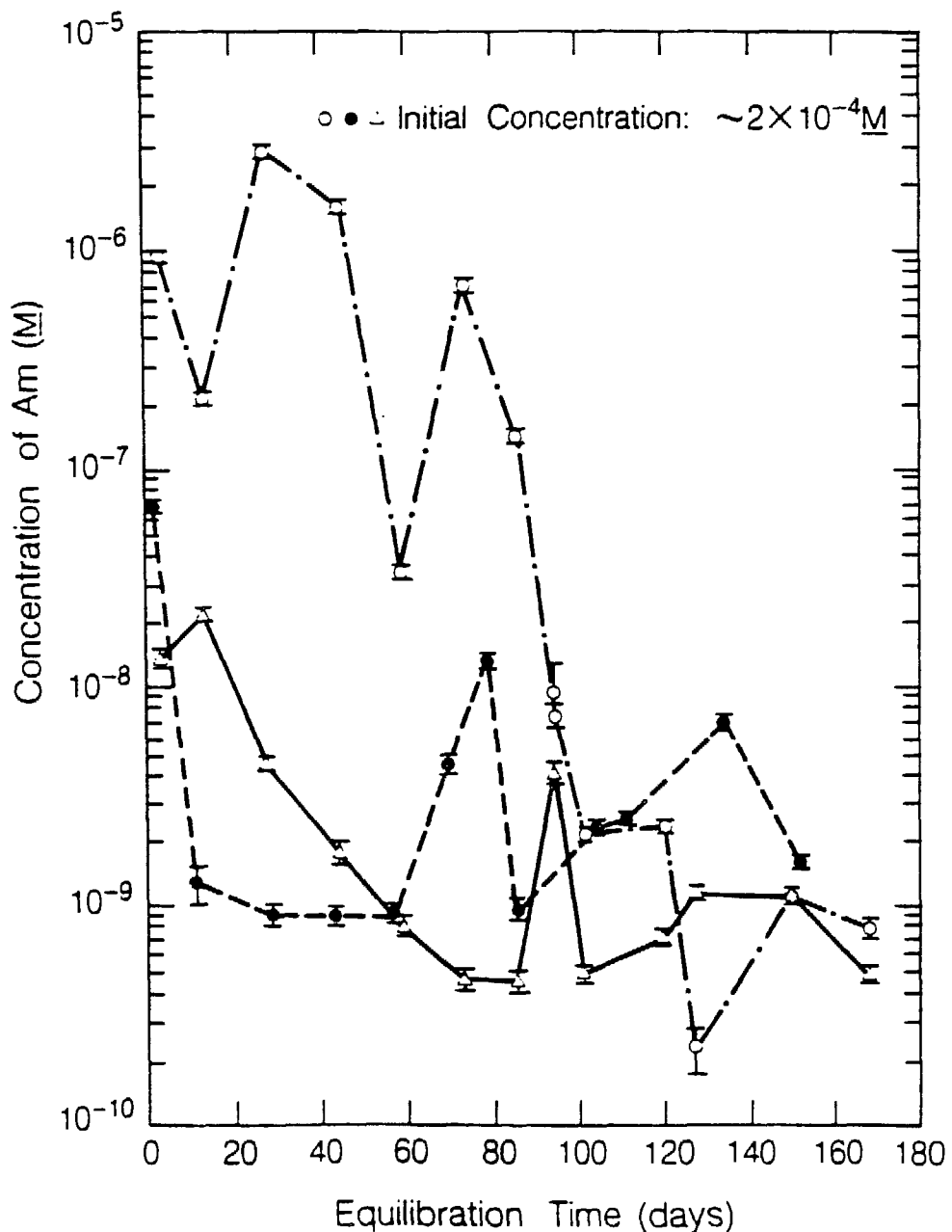


Figure 20. Solution concentration of  $^{243}\text{Am}$  in contact with precipitate obtained from supersaturation in J-13 groundwater at  $60^\circ\text{C}$  as a function of time.  $\text{pH } 5.9 \pm 0.1$  (open circles),  $\text{pH } 7.0 \pm 0.1$  (filled circles), and  $\text{pH } 8.5 \pm 0.1$  (triangles). The americium was added (day 0) as  $\text{Am}^{3+}$ .

toward solubility determinations using less solid phase to minimize the  $\alpha$ -radiation field. We plan to derive steady-state concentrations from frequent samplings during early stages of the experiment before container pitting can occur, providing precipitation kinetics allow this approach. We outline an alternate method to solve this problem in section 1.2. (Recommendation 3.).

#### **5.2.3.2. Oxidation State Determination**

No oxidation state determination was made, because trivalent americium is known to be oxidatively stable under these conditions.

#### **5.2.3.3. Identification of Solids**

The solids were analyzed by x-ray powder diffraction. Powder patterns of the crystalline solids are summarized in Table XV. The solids at pH 7.0 and pH 8.5 were identified as  $\text{AmOHCO}_3$ . The precipitate formed at pH 5.9, however, is neither  $\text{AmOHCO}_3$  nor  $\text{Am(OH)}_3$  and it remains unidentified. This solid is currently being analyzed by NAA at LANL. We hope to obtain the solid's stoichiometry from these measurements. When the sample is returned, we will also use FTIR analysis to further characterize this precipitate.

**Table XV. X-ray powder diffraction patterns of Am solid phases in J-13 groundwater at 60°C, pH 5.9 (phase 1), pH 7.0 (phase 2), and pH 8.4 (phase 3).**

phase 1		phase 2		phase 3	
d(Å)	I <sup>a</sup>	d(Å)	I <sup>a</sup>	d(Å)	I <sup>a</sup>
4.85	s	5.49	m	4.29	vs
3.53	vs	4.94	t	3.67	s
3.05	w+	4.28	vs	3.31	w-
3.01	m	3.67	vs	2.91	w-
2.86	vs	3.31	m	2.63	t
2.47	t	2.92	s	2.48	t
2.43	w-	2.74	t	2.31	t
2.27	t	2.64	w+	1.98	t
2.08	t	2.48	w-	1.92	t
2.04	m	2.40	w-		
2.00	s	2.32	m		
1.88	m	2.05	w+		
1.77	w-	1.99	s		
1.73	t	1.93	w+		
1.66	m	1.84	t		
1.56	w-	1.80	t		
1.47	t	1.69	t		
1.43	t	1.66	w+		
1.33	t				
1.29	w-	1.47	t		
1.27	t				

(a) Relative intensities visually estimated vs = very strong, s = strong, m = medium, w = weak, t = trace.

### 5.3. References

0. D. J. Brooks and J. A. Corrado, "Determination of Radionuclide Solubility in Groundwater for Assessment of High-Level Waste Isolation", U.S. Nuclear Regulatory Commission, Technical Position, Washington, D.C. (1984).
1. H. Nitsche and N. M. Edelstein, "Solubilities and Speciation of Selected Transuranium Ions. A comparison of a Non-Complexing Solution with a Groundwater from the Nevada Tuff Site," *Radiochim Acta* **39**, 23 (1985).
2. A. E. Ogard and J. F. Kerrisk, "Groundwater Chemistry Along the Flow Path between a Proposed Repository Site and the Accessible Environment," Los Alamos National Laboratory report LA-10188-MS, New Mexico (1984).
3. S. L. Phillips, C. A. Phillips, and J. Skeen, "Hydrolysis, Formation and Ionization Constants at 25°C, and at High Temperature - High Ionic Strength," Report LBL-14996, Lawrence Berkeley Laboratory, University of California, Berkeley, California (1985).
4. D. B. Tucker, E. M. Standifer, H. Nitsche, and R. J. Silva, "Data Acquisition and Feedback Control System for Solubility Studies of Nuclear Waste Elements," Report LBL-23451, Lawrence Berkeley Laboratory, University of California, Berkeley, California (1987).
5. E. M. Standifer, S. C. Lee, and H. Nitsche, "Separation of Soluble Transuranium Species from Particulates in Groundwater by Ultrafiltration," Report LBL-23378, Lawrence Berkeley Laboratory, University of California, Berkeley, California (1987).
6. S. C. Lee, R. C. Gatti, and H. Nitsche, "Indirect Determination of Plutonium at Trace Levels by Use of Gamma- and  $L$  x-ray Spectroscopy", Report LBL-23379, Lawrence Berkeley Laboratory, University of California, Berkeley, California (1987).

7. R. M. Garrels, Mineral Equilibria at low Temperature and Pressure, Harper and Brothers, New York, N.Y. (1960).
8. D. Langmuir, "Eh-pH Determinations," in Procedures in Sedimentary Petrology, R. E. Carver, ed., 597-635, Wiley, New York, N.Y. (1971).
9. Y. F. Volkov, G. I. Visyashcheva, and I. I. Kapshukov, "Study of Carbonate Compounds of Pentavalent Actinides with Alkali Metal Cations. V. Production and Identification of Hydrate Forms of Sodium Monocarbonato-neptunylate," Sov. Radiochem. (Eng. transl.) **19**, 263 (1977).
10. Y. F. Volkov, S. V. Tomilin, G. I. Visyashcheva, and I. I. Kapshukov, "Carbonate Compounds of Pentavalent Actinoids with Alkali-Metal Cations. VI. X-Ray Structure Analysis of  $\text{LiNpO}_2\text{CO}_3$  and  $\text{NaNpO}_2\text{CO}_3$ ," Sov. Radiochem. (Eng. transl.) **21**, 579 (1979).
11. Y. F. Volkov, G. I. Visyashcheva, S. V. Tomilin, V. I. Spiriyakov, I. I. Kapshukov, and A. G. Rykov, "Carbonate Compounds of Pentavalent Actinides with Alkali Metal Cations VII. Synthesis and Crystal Structure of Hydrate Compounds with the Composition  $\text{Na}_{0.6}\text{NpO}_2(\text{CO}_3)_{0.8} \cdot n\text{H}_2\text{O}$ ," Sov. Radiochem. (Eng. transl.) **21**, 583 (1979).
12. Y. F. Volkov, G. I. Visyashcheva, S. V. Tomilin, I. I. Kapshukov, and R. G. Rykov, "Study of Carbonate Compounds of Pentavalent Actinides with Alkali-Metal Cations. VIII. Synthesis and X-Ray Diffraction Investigation of Several Compounds of Neptunium(V) with Sodium and Rubidium," Sov. Radiochem. (Eng. transl.) **23**, 191 (1981).
13. K. Nakamoto, Infrared and Raman Spectra of Inorganic and Coordination Compounds, Wiley, New York, N.Y. (1986).
14. L. H. Jones and R. A. Penneman, "Infrared Spectra and Structure of Uranyl and Transuranium (V) and (VI) Ions in Aqueous Perchloric Acid Solution," J. Chem.

Phys. **21**, 542 (1952).

15. H. Nitsche, S. C. Lee, and R. C. Gatti, "Determination of Plutonium Oxidation States at Trace Levels Pertinent to Nuclear Waste Disposal," Report LBL-23158, Lawrence Berkeley Laboratory, University of California, Berkeley, California (1987), *J. Radioanal. Chem.*, in press.
16. L. M. Toth and H. A. Friedman, "The IR Spectrum of Pu(IV) Polymer," *J. Inorg. Nucl. Chem.* **40**, 807 (1978).
17. T. W. Newton, Los Alamos National Laboratory, private communication (1985).
18. I. Y. Starik and F. L. Ginzberg, "The Colloidal Behavior of Americium," *Sov. Radiochem.* **3**, 179 (1961).
19. D. Cohen and A. J. Walter, "Neptunium Pentoxide," *J. Chem. Soc.*, 2696 (1964).
20. T. K. Keenan and F. H. Kruse, "Potassium Double Carbonates of Pentavalent Neptunium, Plutonium, and Americium," *Inorg. Chem.* **3**, 1231 (1964).

## 6. WORK IN PROGRESS

The unidentified solids formed in J-13 groundwater at 60°C are currently analyzed at LANL by NAA. The results will help identify the stoichiometry of these solids. Upon their return, we will further characterize them by FTIR spectroscopy. We also plan to study all unidentified solids from the 90°C study by NAA.

No conclusive results were gained from the americium solubility study at 60°C. Possible reasons for this problem were discussed in section 5.2.3.1 of this report. Should this experiment be repeated using the faster sampling rate as described earlier or should the maximum solution concentrations gained for each individual pH serve as an upper solubility limit?

## 7. REPORTS/PUBLICATIONS/PRESENTATIONS

### 7.1. Reports

During the reporting period we issued 24 Monthly Letter Reports (NNWSI-LBL-LR-01, R0 through NNWSI-LBL-LR-24, R0) and 8 Quarterly Technical Progress Reports (NNWSI-LBL-PR 01, R0 through NNWSI-LBL-PR 08, R0). We also issued the following LBL reports:

- 1) LBL-23158, H. Nitsche, S. C. Lee, and R. C. Gatti "Determination of Plutonium Oxidation States at Trace Levels Pertinent to Nuclear Waste Disposal," 25 pages (1987);
- 2) LBL-23378, E. M. Standifer, S. C. Lee, and H. Nitsche "Separation of Soluble Transuranium Species from Particulates in Groundwater by Ultrafiltration," 14 pages (1987);

- 3) LBL-23379, S. C. Lee, R. C. Gatti, and H. Nitsche "Indirect Determination of Plutonium at Trace Levels by Use of Gamma- and  $L$  x-ray Spectroscopy," 15 pages (1987);
- 4) LBL-23541, D. B. Tucker, E. M. Standifer, R. J. Silva, and H. Nitsche, "Data Acquisition and Feedback Control System for Solubility Studies of Nuclear Waste Elements," 17 pages (1987).

We prepared a Study Plan titled "Determination of Solubilities and Speciation of Waste Radionuclides".

Furthermore, we drafted the Detailed Procedure "Data Acquisition and Feedback Control System for Solubility Studies"; it underwent LANL NNWSI QA Review. We are finalizing the revised version incorporating the reviewer's comments.

Finally, we prepared this letter report (R707, 70 pages) during the reporting period.

## 7.2. Publications

The report LBL-23158 was accepted for publication in the Journal of Radioanalytical Chemistry. We will submit the reports LBL-23378 and LBL-23979 to the Journal of Analytical Chemistry upon their return from NNWSI Policy Review. Soon we will submit the report LBL-23379 to NNWSI Policy Review and then to open literature.

## 7.3. Presentations

We presented three conference papers. The paper "Determination of Plutonium Oxidation States at Trace Levels Pertinent to Nuclear Waste Disposal" by H. Nitsche, S. C. Lee, and R. C. Gatti was presented at the International Conference on Methods and Applications of Radioanalytical Chemistry at Kona, Hawaii, April 5-10, 1987.

The papers "Indirect Determination of Plutonium at Trace Levels by Use of Gamma and  $L$  X-Ray Spectroscopy" by S. C. Lee, R. C. Gatti, and H. Nitsche and "Separation of Soluble Transuranium Species from Particulates in Groundwater by Ultrafiltration" by E. M. Standifer, S. C. Lee, and H. Nitsche were presented at the 193rd ACS National Meeting in Denver, Colorado, April 5-10, 1987. The first named authors gave the presentations.

H. Nitsche gave an invited seminar titled "Temperature Effects in the Solubility and Speciation of Americium" on March 21, 1986, at the United States Department of the Interior, Geological Survey, Denver, Colorado. H. Nitsche talked on the "Temperature Effects on the Solubility and Speciation of Selected Actinides" during a presentation at LANL in the NNWSI Seminar Series on April 1, 1986.

LBL held two invited seminars. The first guest was Dr. Hans Wanner of the Organisation for Economic Co-Operation and Development (OECD), Nuclear Energy Agency (NEA), Paris. On September 8, 1986, he presented the talk "The NEA Thermochemical Data Base - Need and Limitations of Thermodynamic Data for Modeling of Geochemical Processes". The second guest was Dr. Francois David of the University of Paris-Sud, Institut de Physique Nucleaire, Paris. He spoke on September 11, 1987, on the "Structure of Trivalent Lanthanide and Actinide Aquo Ions."

## 8. QUALITY ASSURANCE

The research effort "Solubility and Speciation of Waste Radionuclides Pertinent to Geologic Disposal at Yucca Mountain" conducted at LBL is assigned to DOE-NNWSI Quality Level 1. During the reporting period a Level 1 Quality Assurance Program was initiated and executed at LBL for this effort. We set up a duplicate record system at LANL and we completed a record turnover covering the period from October 1, 1985 to February 23, 1987. LANL Auditors conducted three separate Quality Assurance Surveys (Audits) of this project at LBL. They were held on

November 7, 1985, on October 28-29, 1986, and on August 17-18, 1987. The surveys found that the LBL research is technically and QA-programmatically acceptable for the Nevada Nuclear Waste Storage Investigations (NNWSI).